Active Filter Design Techniques

16.1 Introduction

What is a filter?

> *A filter is a device that passes electric signals at certain frequencies or frequency ranges while preventing the passage of others.*

> **Webster**

Filter circuits are used in a wide variety of applications. In the field of telecommunication, band-pass filters are used in the audio frequency range (0–20 kHz) for modems and speech processing. High-frequency band-pass filters (several hundred MHz) are used for channel selection in telephone central offices. Data acquisition systems usually require antialiasing low-pass filters as well as low-pass noise filters in their preceding signal-conditioning stages. System power supplies often use band-rejection filters to suppress the 60 Hz line frequency and high-frequency transients.

In addition, there are filters that do not filter any frequencies of a complex input signal, but just add a linear phase shift to each frequency component, thus contributing to a constant time delay. These are called all-pass filters.

At high frequencies (>1 MHz), all of these filters usually consist of passive components such as inductors (L), resistors (R), and capacitors (C). They are then called LRC filters.

In the lower frequency range (1 Hz–1 MHz), however, the inductor value becomes very large and the inductor itself gets quite bulky, making economical production difficult.

In these cases, active filters become important. Active filters are circuits that use an operational amplifier (op amp) as the active device in combination with some resistors and capacitors to provide an LRC-like filter performance at low frequencies (Fig. 16.1).

This chapter covers active filters. It introduces the three main filter optimizations (Butterworth, Tschebyscheff, and Bessel), followed by five sections describing the most common active filter applications: low-pass, high-pass, band-pass, band-rejection, and all-pass filters. Rather than resembling just another filter book, the individual filter sections are written in a cookbook style, thus avoiding tedious mathematical derivations that are covered in books devoted to the subject of active filter design. Each section starts with the general transfer function of a filter,
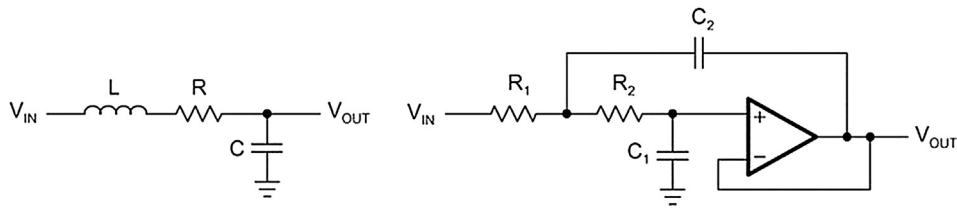
Figure 16.1
Second-order passive low-pass and second-order active low-pass.

followed by the design equations to calculate the individual circuit components. The chapter closes with a section on practical design hints for single-supply filter designs.

If you find this material to be complex, the following chapter introduces techniques that will allow you to very quickly design working filters with a minimum of mathematical calculation. What is lost, though with the rapid techniques in the following chapter is the ability to design every combination of gain, frequency, and quality factor—it makes certain decisions up front that simplify the process. If you need a specialized filter, stick with the techniques in this chapter.

16.2 Fundamentals of Low-Pass Filters

The most simple low-pass filter is the passive RC low-pass network shown in Fig. 16.2.

Its transfer function is

$$A(s) = \frac{\frac{1}{RC}}{s + \frac{1}{RC}} = \frac{1}{1 + sRC}$$

where the complex frequency variable, $s = j\omega + \sigma$, allows for any time variable signals. For pure sine waves, the damping constant, σ, becomes zero and $s = j\omega$.

For a normalized presentation of the transfer function, s is referred to the filter's corner frequency, or -3 dB frequency, ω_C, and has these relationships:
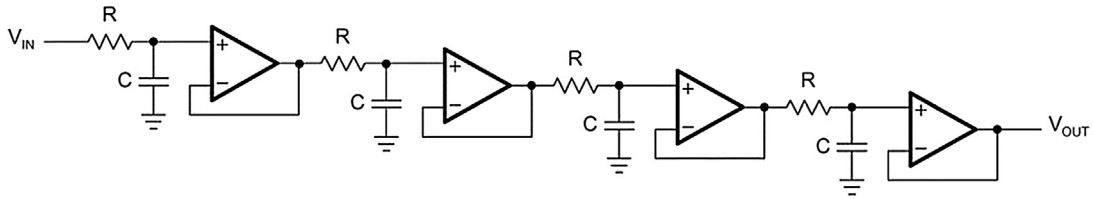
$$s = \frac{s}{\omega_C} = \frac{j\omega}{\omega_C} = j\frac{f}{f_C} = j\Omega$$

With the corner frequency of the low-pass in Fig. 16.2 being $f_C = 1/2\pi RC$, s becomes $s = sRC$ and the transfer function A(s) results in:

$$A(s) = \frac{1}{1 + s}$$
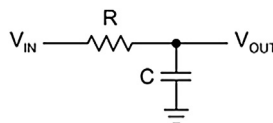
Figure 16.2
First-order passive RC low-pass.

Figure 16.3
Fourth-order passive RC low-pass with decoupling amplifiers.

The magnitude of the gain response is

$$|A| = \frac{1}{\sqrt{1 + \Omega^2}}$$

For frequencies $\Omega \gg 1$, the rolloff is 20 dB/decade. For a steeper rolloff, n filter stages can be connected in series as shown in Fig. 16.3. To avoid loading effects, op amps, operating as impedance converters, separate the individual filter stages.

The resulting transfer function is

$$A(s) = \frac{1}{(1 + \alpha_1 s)(1 + \alpha_2 s)...(1 + \alpha_n s)}$$

In the case that all filters have the same cut-off frequency, f_C, the coefficients become $\alpha_1 = \alpha_2 = ...\alpha_n = \alpha = \sqrt{\sqrt[n]{2} - 1}$, and f_C of each partial filter is $1/\alpha$ times higher than f_C of the overall filter.

Fig. 16.4 shows the results of a fourth-order RC low-pass filter. The rolloff of each partial filter (Curve 1) is -20 dB/decade, increasing the rolloff of the overall filter (Curve 2) to 80 dB/decade.

The corner frequency of the overall filter is reduced by a factor of $\alpha \approx 2.3$ times versus the -3 dB frequency of partial filter stages.

In addition, Fig. 16.4 shows the transfer function of an ideal fourth-order low-pass function (Curve 3).

In comparison to the ideal low-pass, the RC low-pass lacks in the following characteristics:

- The passband gain varies long before the corner frequency, f_C, thus amplifying the upper passband frequencies less than the lower passband.
- The transition from the passband into the stopband is not sharp, but happens gradually, moving the actual 80-dB rolloff by 1.5 octaves above f_C.
- The phase response is not linear, thus increasing the amount of signal distortion significantly.
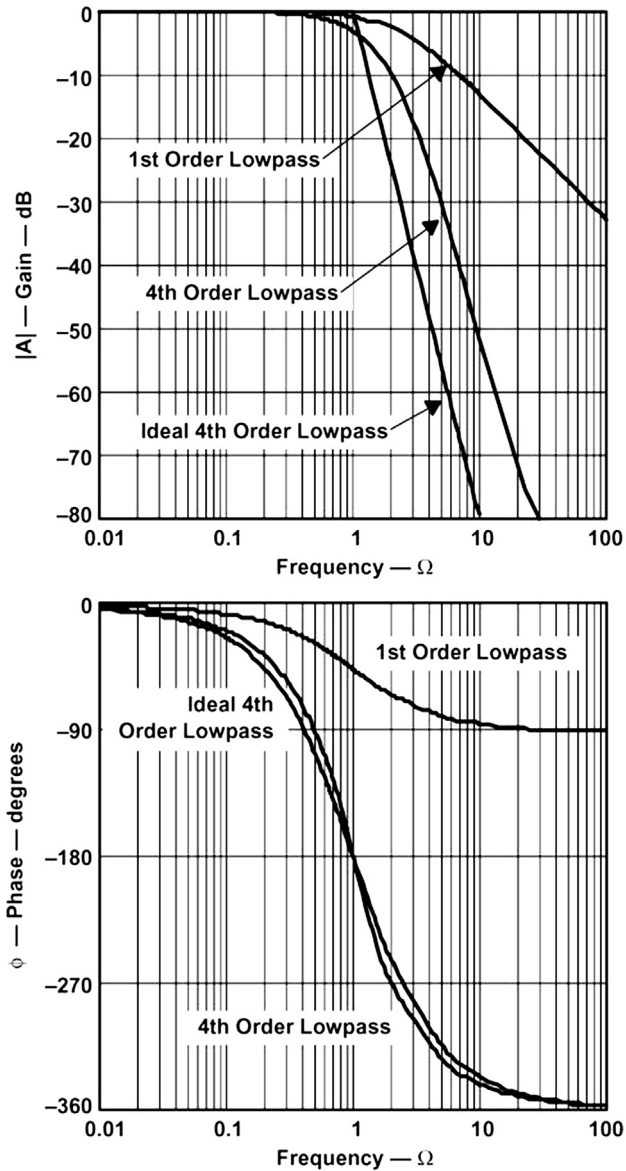
Figure 16.4
Frequency and phase responses of a fourth-order passive RC low-pass filter.
Note: Filter response graphs plot gain versus the normalized frequency axis $\Omega(\Omega = f/f_C)$. Curve 1: first-order partial low-pass filter, Curve 2: fourth-order overall low-pass filter, Curve 3: ideal fourth-order low-pass filter.

The gain and phase response of a low-pass filter can be optimized to satisfy *one* of the following three criteria:

1. a maximum passband flatness,
2. an immediate passband-to-stopband transition, and
3. a linear phase response.

For that purpose, the transfer function must allow for complex poles and needs to be of the following type:

$$A(s) = \frac{A_0}{(1 + a_1s + b_1s^2)(1 + a_2s + b_2s^2)...(1 + a_ns + b_ns^2)} = \frac{A_0}{\prod_i (1 + a_is + b_is^2)}$$

where A_0 is the passband gain at DC, and a_i and b_i are the filter coefficients.

Since the denominator is a product of quadratic terms, the transfer function represents a series of cascaded second-order low-pass stages, with a_i and b_i being positive real coefficients. These coefficients define the complex pole locations for each second-order filter stage, thus determining the behavior of its transfer function.

The following three types of predetermined filter coefficients are available and listed in table format in Section 16.9:

- The Butterworth coefficients, optimizing the passband for maximum flatness.
- The Tschebyscheff coefficients, sharpening the transition from passband into the stopband.
- The Bessel coefficients, linearizing the phase response up to f_C.

The transfer function of a passive RC filter does not allow further optimization, due to the lack of complex poles. The only possibility to produce conjugate complex poles using passive components is the application of LRC filters. However, these filters are mainly used at high frequencies. In the lower frequency range (<10 MHz) the inductor values become very large and the filter becomes uneconomical to manufacture. In these cases active filters are used.

Active filters are RC networks that include an active device, such as an operational amplifier (op amp).

Section 16.3 shows that the products of the RC values and the corner frequency must yield the predetermined filter coefficients a_i and b_i, to generate the desired transfer function.

The following paragraphs introduce the most commonly used filter optimizations.

16.2.1 Butterworth Low-Pass Filters

The Butterworth low-pass filter provides maximum passband flatness. Therefore, a Butterworth low-pass is often used as antialiasing filter in data converter applications where precise signal levels are required across the entire passband.

Fig. 16.5 plots the gain response of different orders of Butterworth low-pass filters versus the normalized frequency axis, $\Omega(\Omega = f/f_C)$; the higher the filter order, the longer the passband flatness.

16.2.2 Tschebyscheff Low-Pass Filters

The Tschebyscheff low-pass filters provide an even higher gain rolloff above f_C. However, as Fig. 16.6 shows, the passband gain is not monotone, but contains ripples of constant magnitude instead. For a given filter order, the higher the passband ripples, the higher the filter's rolloff.

With increasing filter order, the influence of the ripple magnitude on the filter rolloff diminishes.

Each ripple accounts for one second-order filter stage. Filters with even order numbers generate ripples above the 0-dB line, whereas filters with odd order numbers create ripples below 0 dB.
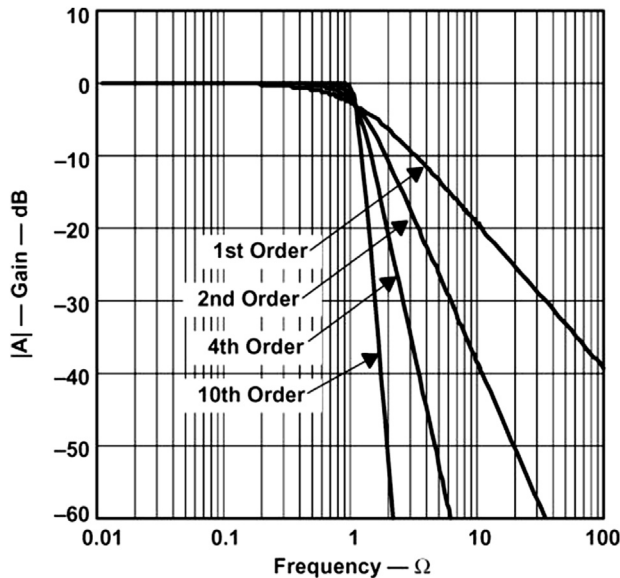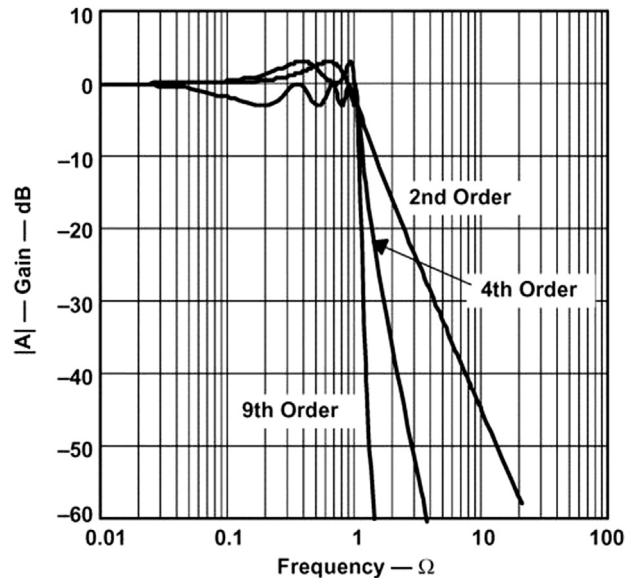

Figure 16.5
Amplitude responses of Butterworth low-pass filters.

Figure 16.6
Gain responses of Tschebyscheff low-pass filters.

Tschebyscheff filters are often used in filter banks, where the frequency content of a signal is of more importance than a constant amplification.

16.2.3 Bessel Low-Pass Filters

The Bessel low-pass filters have a linear phase response (Fig. 16.7) over a wide frequency range, which results in a constant group delay (Fig. 16.8) in that frequency range. Bessel low-pass filters, therefore, provide an optimum square-wave transmission behavior. However, the passband gain of a Bessel low-pass filter is not as flat as that of the Butterworth low-pass, and the transition from passband to stopband is by far not as sharp as that of a Tschebyscheff low-pass filter (Fig. 16.9).

16.2.4 Quality Factor Q

The quality factor Q is an equivalent design parameter to the filter order n. Instead of designing an nth order Tschebyscheff low-pass, the problem can be expressed as designing a Tschebyscheff low-pass filter with a certain Q.

For band-pass filters, Q is defined as the ratio of the mid-frequency, f_m, to the bandwidth at the two −3 dB points:
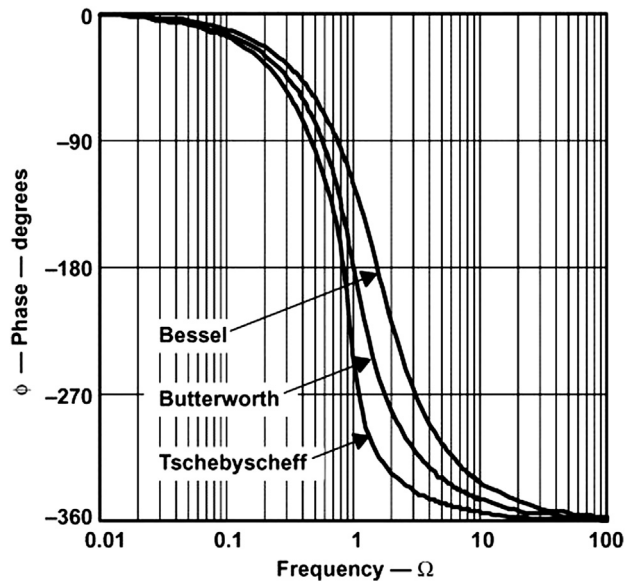
$$Q = \frac{f_m}{(f_2 - f_1)}$$

Figure 16.7
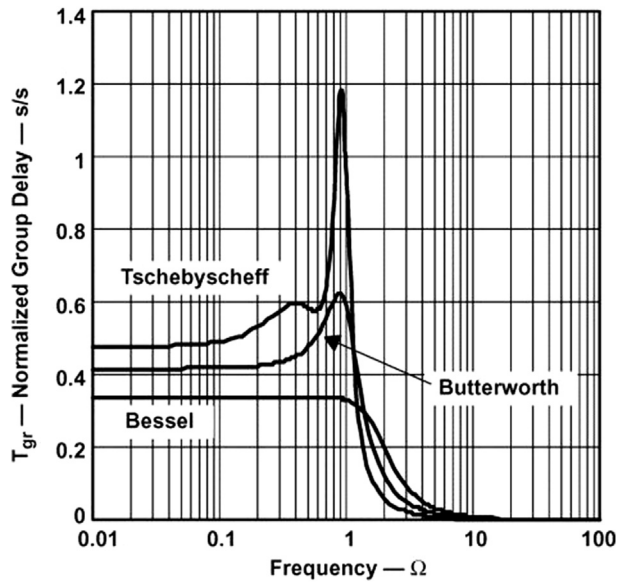Comparison of phase responses of fourth-order low-pass filters.

Figure 16.8
Comparison of normalized group delay (t_{gr}) of fourth-order low-pass filters.
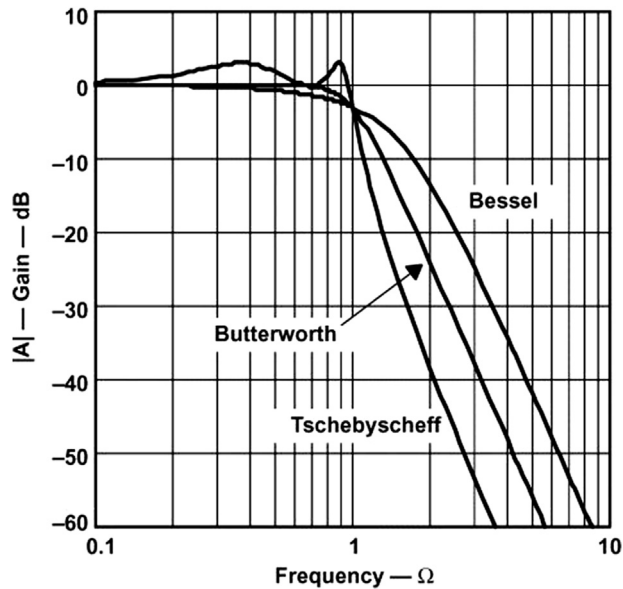
Figure 16.9
Comparison of gain responses of fourth-order low-pass filters.

For low-pass and high-pass filters, Q represents the pole quality and is defined as:

$$Q = \frac{\sqrt{b_i}}{a_i}$$

High Qs can be graphically presented as the distance between the 0 dB line and the peak point of the filter's gain response. An example is given in Fig. 16.10, which shows a 10th-order Tschebyscheff low-pass filter and its five partial filters with their individual Qs.

The gain response of the fifth filter stage peaks at 31 dB, which is the logarithmic value of Q_5:

$$Q_5[\text{dB}] = 20 \, \text{log} Q_5$$

Solving for the numerical value of Q_5 yields

$$Q_5 = 10 \, \frac{31}{20} = 35.48$$

which is within 1% of the theoretical value of $Q = 35.85$ given in Section 16.9, Table 16.11, last row.

The graphical approximation is good for $Q > 3$. For lower Qs, the graphical values differ from the theoretical value significantly. However, only higher Qs are of concern, since the higher the Q is, the more a filter inclines to instability.
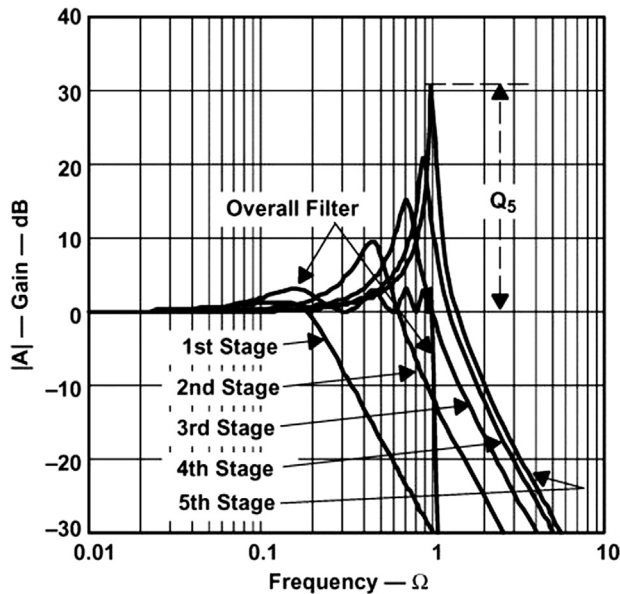
Figure 16.10
Graphical presentation of quality factor Q on a 10th-order Tschebyscheff low-pass filter.

16.2.5 Summary

The general transfer function of a low-pass filter is:

$$A(s) = \frac{A_0}{\prod_i (1 + a_i s + b_i s)} \tag{16.1}$$

The filter coefficients a_i and b_i distinguish between Butterworth, Tschebyscheff, and Bessel filters. The coefficients for all three types of filters are tabulated down to the 10th-order in Section 16.9, Tables 16.6 through 16.12.

The multiplication of the denominator terms with each other yields an nth order polynomial of s, with n being the filter order.

While n determines the gain rolloff above f_C with $n \cdot 20$ dB/decade, a_i and b_i determine the gain behavior in the passband.

In addition, the ratio $\frac{\sqrt{b_i}}{a_i} = Q$ is defined as the pole quality. The higher the Q value, the more a filter inclines to instability.

16.3 Low-Pass Filter Design

Eq. (16.1) represents a cascade of second-order low-pass filters. The transfer function of a single stage is

$$A_i(s) = \frac{A_0}{(1 + a_i s + b_i s^2)} \tag{16.2}$$

For a first-order filter, the coefficient b is always zero ($b_1 = 0$), thus yielding:

$$A(s) = \frac{A_0}{1 + a_1 s} \tag{16.3}$$

The first-order and second-order filter stages are the building blocks for higher-order filters.

Often the filters operate at unity gain ($A_0 = 1$) to lessen the stringent demands on the op amp's open-loop gain.

Fig. 16.11 shows the cascading of filter stages up to the sixth order. A filter with an even order number consists of second-order stages only, while filters with an odd order number include an additional first-order stage at the beginning.

Fig. 16.10 demonstrated that the higher the corner frequency of a partial filter, the higher its Q. Therefore, to avoid the saturation of the individual stages, the filters need to be placed in the order of rising Q values. The Q values for each filter order are listed (in rising order) in Section 16.9, Tables 16.6 through 16.12.
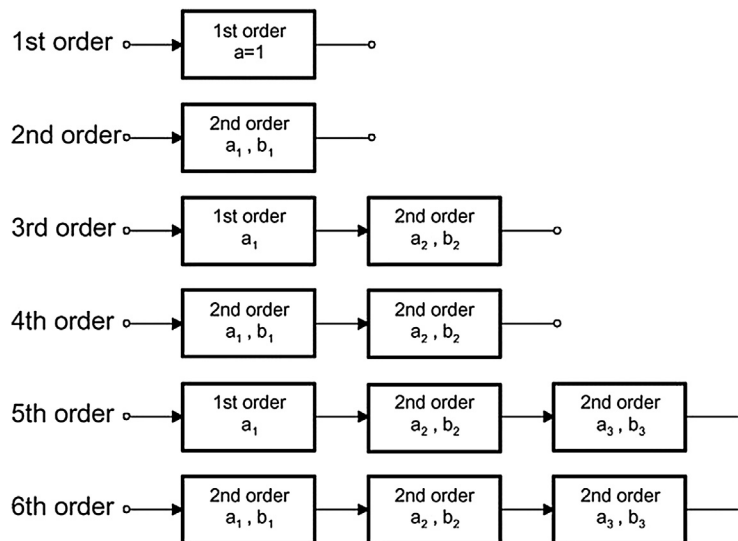
Figure 16.11
Cascading filter stages for higher-order filters.

16.3.1 First-Order Low-Pass Filter

Figs. 16.12 and 16.13 show a first-order low-pass filter in the inverting and in the noninverting configuration.

The transfer functions of the circuits are given as:

$$A(s) = \frac{1 + \dfrac{R_2}{R_3}}{1 + \omega_c R_1 C_1 s} \quad \text{and} \quad A(s) = \frac{-\dfrac{R_2}{R_1}}{1 + \omega_c R_2 C_1 s}$$

The negative sign indicates that the inverting amplifier generates a 180 degrees phase shift from the filter input to the output.

The coefficient comparison between the two transfer functions and Eq. (16.3) yields
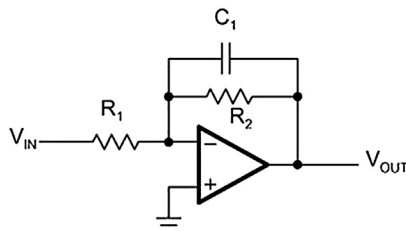
$$A_0 = 1 + \frac{R_2}{R_3} \quad \text{and} \quad A_0 = -\frac{R_2}{R_1}$$

$$a_1 = \omega_c R_1 C_1 \quad \text{and} \quad a_1 = \omega_c R_2 C_1$$
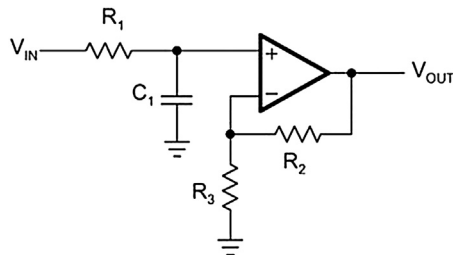
Figure 16.12
First-order noninverting low-pass filter.

Figure 16.13
First-order inverting low-pass filter.

To dimension the circuit, specify the corner frequency (f_C), the DC gain (A_0), and capacitor C_1, and then solve for resistors R_1 and R_2:

$$R_1 = \frac{a_1}{2\pi f_c C_1} \quad \text{and} \quad R_2 = \frac{a_1}{2\pi f_c C_1}$$

$$R_2 = R_3(A_0 - 1) \quad \text{and} \quad R_1 = -\frac{R_2}{A_0}$$

The coefficient a_1 is taken from one of the coefficient tables, Tables 16.6 through 16.12 in Section 16.9.

Note, that all filter types are identical in their first order and $a_1 = 1$. For higher filter orders, however, $a_1 \neq 1$ because the corner frequency of the first-order stage is different from the corner frequency of the overall filter.

Example 16.1. First-Order Unity-Gain Low-Pass Filter.

For a first-order unity-gain low-pass filter with $f_C = 1$ kHz and $C_1 = 47$ nF, R_1 calculates to:

$$R_1 = \frac{a_1}{2\pi f_c C_1} = \frac{1}{2\pi \cdot 10^3 \text{ Hz} \cdot 47 \cdot 10^{-9} \text{ F}} = 3.38 \text{ k}\Omega$$

However, to design the first stage of a third-order unity-gain Bessel low-pass filter, assuming the same values for f_C and C_1, requires a different value for R_1. In this case, obtain a_1 for a third-order Bessel filter from Table 16.6 in Section 16.9 (Bessel coefficients) to calculate R_1:

$$R_1 = \frac{a_1}{2\pi f_c C_1} = \frac{0.756}{2\pi \cdot 10^3 \text{ Hz} \cdot 47 \cdot 10^{-9} \text{ F}} = 2.56 \text{ k}\Omega$$

When operating at unity gain, the noninverting amplifier reduces to a voltage follower (Fig. 16.14), thus inherently providing a superior gain accuracy. In the case of the inverting amplifier, the accuracy of the unity gain depends on the tolerance of the two resistors, R_1 and R_2.
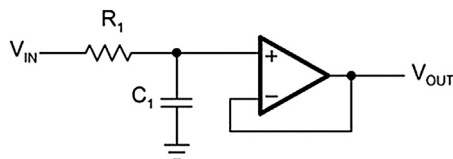
Figure 16.14
First-order noninverting low-pass filter with unity gain.

16.3.2 Second-Order Low-Pass Filter

There are two topologies for a second-order low-pass filter, the Sallen−Key and the multiple feedback (MFB) topology.

16.3.2.1 Sallen−Key Topology

The general Sallen−Key topology in Fig. 16.15 allows for separate gain setting via $A_0 = 1 + R_4/R_3$. However, the unity-gain topology in Fig. 16.16 is usually applied in filter designs with high-gain accuracy, unity gain, and low Qs (Q < 3).

The transfer function of the circuit in Fig. 16.15 is given as:

$$A(s) = \frac{A_0}{1 + \omega_c[C_1(R_1 + R_2) + (1 - A_0)R_1C_2]s + \omega_c^2 R_1 R_2 C_1 C_2 s^2}$$

For the unity-gain circuit in Fig. 16.16 ($A_0 = 1$), the transfer function simplifies to:

$$A(s) = \frac{1}{1 + \omega_c C_1(R_1 + R_2)s + \omega_c^2 R_1 R_2 C_1 C_2 s^2}$$
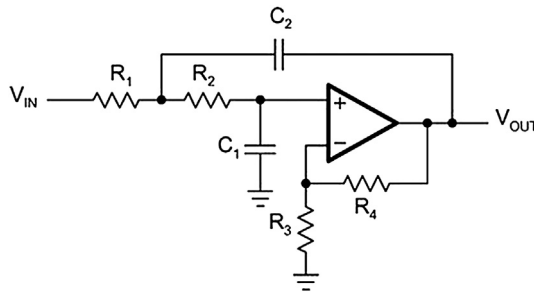
Figure 16.15
General Sallen−Key low-pass filter.
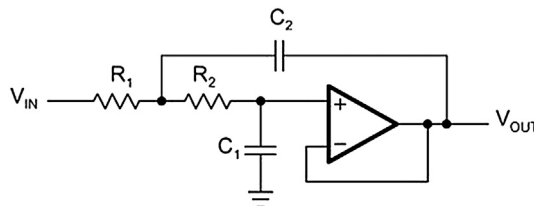
Figure 16.16
Unity-gain Sallen−Key low-pass filter.

The coefficient comparison between this transfer function and Eq. (16.2) yields

$$A_0 = 1$$
$$a_1 = \omega_c C_1 (R_1 + R_2)$$
$$b_1 = \omega_c^2 R_1 R_2 C_1 C_2$$

Given C_1 and C_2, the resistor values for R_1 and R_2 are calculated through:

$$R_{1,2} = \frac{a_1 C_2 \mp \sqrt{a_1^2 C_2^2 - 4 b_1 C_1 C_2}}{4 \pi f_c C_1 C_2}$$

To obtain real values under the square root, C_2 must satisfy the following condition:

$$C_2 \geq C_1 \frac{4 b_1}{a_1^2}$$

Example 16.2. Second-Order Unity-Gain Tschebyscheff Low-Pass Filter.

The task is to design a second-order unity-gain Tschebyscheff low-pass filter with a corner frequency of $f_C = 3$ kHz and a 3-dB passband ripple.

From Table 16.11 (the Tschebyscheff coefficients for 3-dB ripple), obtain the coefficients a_1 and b_1 for a second-order filter with $a_1 = 1.0650$ and $b_1 = 1.9305$.

Specifying C_1 as 22 nF yields in a C_2 of:

$$C_2 \geq C_1 \frac{4 b_1}{a_1^2} = 22.10^{-9} \text{ nF} \cdot \frac{4 \cdot 1.9305}{1.065^2} \cong 150 \text{ nF}$$

Inserting a_1 and b_1 into the resistor equation for $R_{1,2}$ results in:

$$R_1 = \frac{1.065 \cdot 150 \cdot 10^{-9} - \sqrt{(1.065 \cdot 150 \cdot 10^{-9})^2 - 4 \cdot 1.9305 \cdot 22 \cdot 10^{-9} \cdot 150 \cdot 10^{-9}}}{4 \pi \cdot 3 \cdot 10^3 \cdot 22 \cdot 10^{-9} \cdot 150 \cdot 10^{-9}} = 1.26 \text{ k}\Omega$$

and

$$R_2 = \frac{1.065 \cdot 150 \cdot 10^{-9} - \sqrt{(1.065 \cdot 150 \cdot 10^{-9})^2 - 4 \cdot 1.9305 \cdot 22 \cdot 10^{-9} \cdot 150 \cdot 10^{-9}}}{4 \pi \cdot 3 \cdot 10^3 \cdot 22 \cdot 10^{-9} \cdot 150 \cdot 10^{-9}} = 1.30 \text{ k}\Omega$$

with the final circuit shown in Fig. 16.17.

A special case of the general Sallen–Key topology is the application of equal resistor values and equal capacitor values: $R_1 = R_2 = R$ and $C_1 = C_2 = C$.
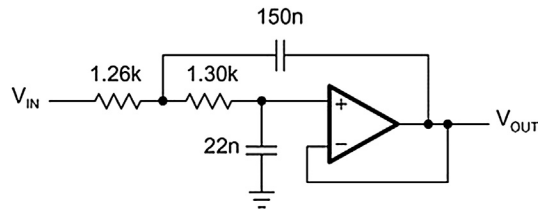
Figure 16.17
Second-order unity-gain Tschebyscheff low-pass with 3 dB ripple.

The general transfer function changes to:

$$A(s) = \frac{A_0}{1 + \omega_c RC(3 - A_0)s + (\omega_c RC)^2 s^2} \quad \text{with} \quad A_0 = 1 + \frac{R_4}{R_3}$$

The coefficient comparison with Eq. (16.2) yields the following:

$$a_1 = \omega RC(3 - A_0)$$
$$b_1 = (\omega RC)^2$$

Given C and solving for R and A_0 results in:

$$R = \frac{\sqrt{b_1}}{2\pi f_c C} \quad \text{and} \quad A_0 = 3 - \frac{a_1}{\sqrt{b_1}} = 3 - \frac{1}{Q}$$

Thus, A_0 depends solely on the pole quality Q and vice versa; Q, and with it the filter type, is determined by the gain setting of A_0:

$$Q = \frac{1}{3 - A_0}$$

The circuit in Fig. 16.18 allows the filter type to be changed through the various resistor ratios R_4/R_3.
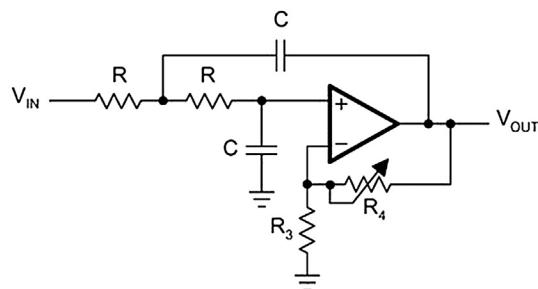
Figure 16.18
Adjustable second-order low-pass filter.

Table 16.1: Second-Order Filter Coefficients

Second-Order	Bessel	Butterworth	3 dB Tschebyscheff
a_1	1.3617	1.4142	1.065
b_1	0.618	1	1.9305
Q	0.58	0.71	1.3
R_4/R_3	0.268	0.568	0.234

Table 16.1 lists the coefficients of a second-order filter for each filter type and gives the resistor ratios that adjust the Q.

16.3.2.2 Multiple Feedback Low Pass Filter Topology

The multiple feedback (MFB) topology is commonly used in filters that have high Qs and require a high gain.

The transfer function of the circuit in Fig. 16.19 is given as follows:

$$A(s) = - \frac{\dfrac{R_2}{R_1}}{1 + \omega_c C_1 \left(R_2 + R_3 + \dfrac{R_2 R_3}{R_1} \right) s + \omega_c^2 C_1 C_2 R_2 R_3 s^2}$$

Through coefficient comparison with Eq. (16.2) one obtains the relation:

$$A_0 = - \frac{R_2}{R_1}$$

$$a_1 = \omega_c C_1 \left(R_2 + R_3 + \frac{R_2 R_3}{R_1} \right)$$

$$b_1 = \omega_c^2 C_1 C_2 R_2 R_3$$

Figure 16.19
Second-order multiple feedback low-pass filter.

Given C_1 and C_2, and solving for the resistors R_1-R_3:
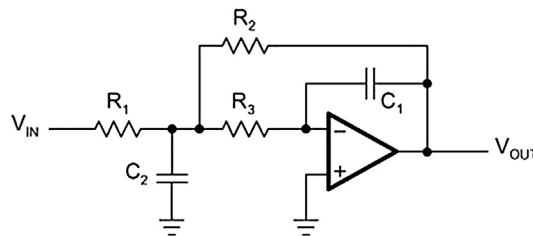
$$R_2 = \frac{a_1 C_2 - \sqrt{a_1^2 C_2^2 - 4b_1 C_1 C_2 (1 - A_0)}}{4\pi f_c C_1 C_2}$$

$$R_1 = \frac{R_2}{-A_0}$$

$$R_3 = \frac{b_1}{4\pi^2 f_c^2 C_1 C_2 R_2}$$

To obtain real values for R_2, C_2 must satisfy the following condition:

$$C_2 \geq C_1 \frac{4b_1 (1 - A_0)}{a_1^2}$$

16.3.3 Higher-Order Low-Pass Filters

Higher-order low-pass filters are required to sharpen a desired filter characteristic. For that purpose, first-order and second-order filter stages are connected in series, so that the product of the individual frequency responses results in the optimized frequency response of the overall filter.

To simplify the design of the partial filters, the coefficients a_i and b_i for each filter type are listed in the coefficient tables (Tables 16.6 through 16.12 in Section 16.9), with each table providing sets of coefficients for the first 10 filter orders.

Example 16.3. Fifth Order Filter (Table 16.2).

The task is to design a fifth-order unity-gain Butterworth low-pass filter with the corner frequency $f_C = 50$ kHz.

First the coefficients for a fifth-order Butterworth filter are obtained from Table 16.7, Section 16.9.

Then dimension each partial filter by specifying the capacitor values and calculating the required resistor values.

Table 16.2: Example 16.3 Filters

	a_i	b_i
Filter 1	$A_1 = 1$	$b_1 = 0$
Filter 2	$a_2 = 1.6180$	$b_2 = 1$
Filter 3	$a_3 = 0.6180$	$b_3 = 1$

16.3.3.1 First Filter

With $C_1 = 1$ nF,

$$R_1 = \frac{a_1}{2\pi f_c C_1} = \frac{1}{2\pi \cdot 50 \cdot 10^3 \text{ Hz} \cdot 1 \cdot 10^{-9} \text{ F}} = 3.18 \text{ k}\Omega$$

The closest 1% value is 3.16 kΩ (See Fig 16.20).

16.3.3.2 Second Filter

With $C_1 = 820$ pF,

$$C_2 \geq C_1 \frac{4b_2}{a_2^2} = 820 \cdot 10^{-12} \text{ F} \cdot \frac{4 \cdot 1}{1.618^2} = 1.26 \text{ nF}$$

The closest 5% value is 1.5 nF (See Fig 16.21).

With $C_1 = 820$ pF and $C_2 = 1.5$ nF, calculate the values for R_1 and R_2 through:

$$R_1 = \frac{a_2 C_2 - \sqrt{a_2^2 C_2^2 - 4b_2 C_1 C_2}}{4\pi f_c C_1 C_2} \quad \text{and} \quad R_1 = \frac{a_2 C_2 + \sqrt{a_2^2 C_2^2 - 4b_2 C_1 C_2}}{4\pi f_c C_1 C_2}$$
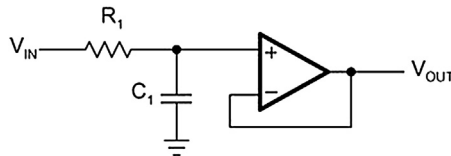
Figure 16.20
First-order unity-gain low-pass.
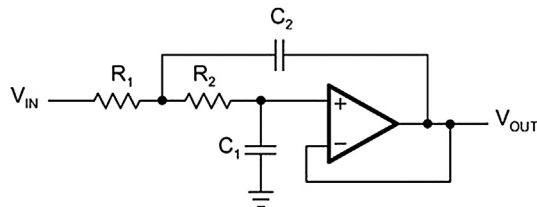
Figure 16.21
Second-order unity-gain Sallen–Key low-pass filter.
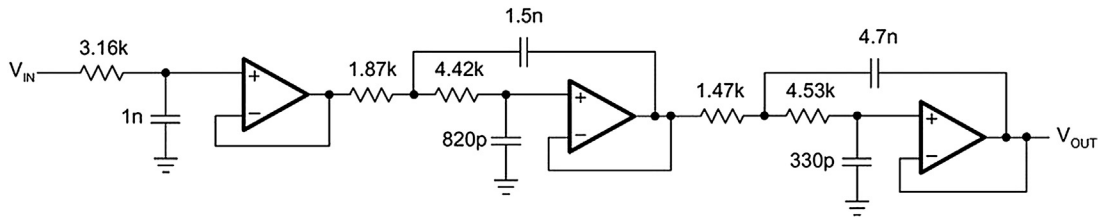
Figure 16.22
Fifth-order unity-gain Butterworth low-pass filter.

and obtain

$$R_1 = \frac{1.618 \cdot 1.5 \cdot 10^{-9} - \sqrt{\left(1.618 \cdot 1.5 \cdot 10^{-9}\right)^2 - 4 \cdot 1 \cdot 820 \cdot 10^{-12} \cdot 1.5 \cdot 10^{-9}}}{4\pi \cdot 50 \cdot 10^3 \cdot 820 \cdot 10^{-12} \cdot 1.5 \cdot 10^{-9}} = 1.87 \text{ k}\Omega$$

$$R_2 = \frac{1.618 \cdot 1.5 \cdot 10^{-9} - \sqrt{\left(1.618 \cdot 1.5 \cdot 10^{-9}\right)^2 - 4 \cdot 1 \cdot 820 \cdot 10^{-12} \cdot 1.5 \cdot 10^{-9}}}{4\pi \cdot 50 \cdot 10^3 \cdot 820 \cdot 10^{-12} \cdot 1.5 \cdot 10^{-9}} = 4.42 \text{ k}\Omega$$

R_1 and R_2 are available 1% resistors.

16.3.3.3 Third Filter

The calculation of the third filter is identical to the calculation of the second filter, except that a_2 and b_2 are replaced by a_3 and b_3, thus resulting in different capacitor and resistor values.

Specify C_1 as 330 pF, and obtain C_2 with:

$$C_2 \geq C_1 \frac{4b_3}{a_3^2} = 330 \cdot 10^{-12} \text{ F} \cdot \frac{4.1}{0.618^2} = 3.46 \text{ nF}$$

The closest 10% value is 4.7 nF.

With $C_1 = 330$ pF and $C_2 = 4.7$ nF, the values for R_1 and R_2 are as follows:

- $R_1 = 1.45$ kΩ, with the closest 1% value being 1.47 kΩ, and
- $R_2 = 4.51$ kΩ, with the closest 1% value being 4.53 kΩ.

Fig. 16.22 shows the final filter circuit with its partial filter stages.

16.4 High-Pass Filter Design

By replacing the resistors of a low-pass filter with capacitors, and its capacitors with resistors, a high-pass filter is created (See Fig. 16.23).
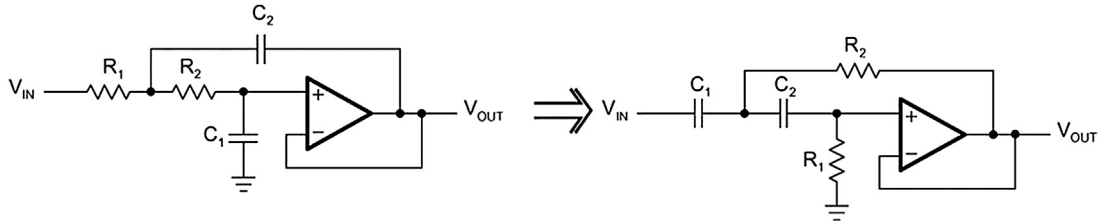
Figure 16.23
Low-pass to high-pass transition through components exchange.

To plot the gain response of a high-pass filter, mirror the gain response of a low-pass filter at the corner frequency, $\Omega = 1$, thus replacing Ω with $1/\Omega$ and S with $1/S$ in Eq. (16.1) (See Fig. 16.24).

The general transfer function of a high-pass filter is then:

$$A(s) = \frac{A_\infty}{\prod\limits_i \left(1 + \dfrac{a_i}{s} + \dfrac{b_i}{s^2}\right)} \tag{16.4}$$

with A_∞ being the passband gain.
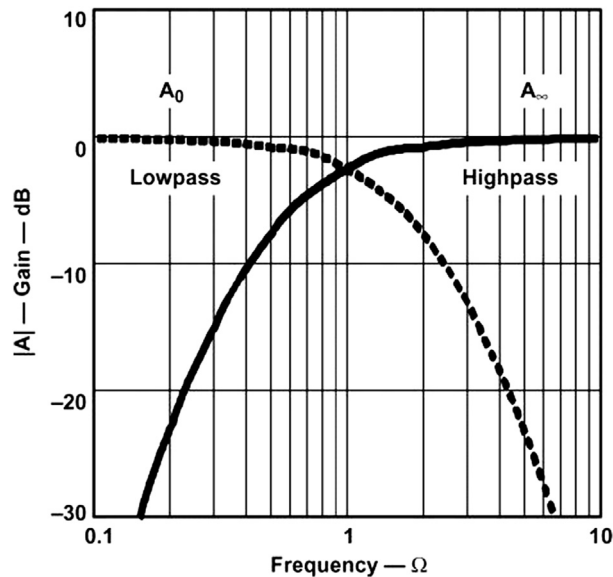
Figure 16.24
Developing the gain response of a high-pass filter.

Since Eq. (16.4) represents a cascade of second-order high-pass filters, the transfer function of a single stage is given as:

$$A_i(s) = \frac{A_\infty}{\left(1 + \dfrac{a_i}{s} + \dfrac{b_i}{s^2}\right)} \tag{16.5}$$

With $b = 0$ for all first-order filters, the transfer function of a first-order filter simplifies to:

$$A(s) = \frac{A_0}{1 + \dfrac{a_i}{s}} \tag{16.6}$$

16.4.1 First-Order High-Pass Filter

Figs. 16.25 and 16.26 show a first-order high-pass filter in the noninverting and the inverting configuration.

The transfer functions of the circuits are as follows:

$$A(s) = \frac{1 + \dfrac{R_2}{R_3}}{1 + \dfrac{1}{\omega_c R_1 C_1} \cdot \dfrac{1}{s}} \quad \text{and} \quad A(s) = -\frac{\dfrac{R_2}{R_1}}{1 + \dfrac{1}{\omega_c R_1 C_1} \cdot \dfrac{1}{s}}$$
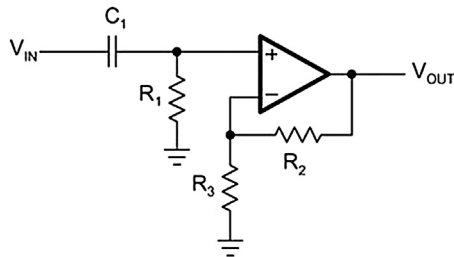
Figure 16.25
First-order noninverting high-pass filter.
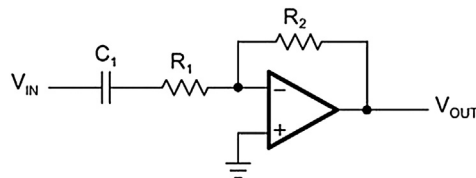
Figure 16.26
First-order inverting high-pass filter.

The negative sign indicates that the inverting amplifier generates a 180°phase shift (from the filter input to the output).

The coefficient comparison between the two transfer functions and Eq. (16.6) provides two different passband gain factors:

$$A_\infty = 1 + \frac{R_2}{R_3} \quad \text{and} \quad A_\infty = -\frac{R_2}{R_1}$$

while the term for the coefficient a_1 is the same for both circuits:

$$a_1 = \frac{1}{\omega_c R_1 C_1}$$

To dimension the circuit, specify the corner frequency (f_C), the DC gain (A_∞), and capacitor (C_1), and then solve for R_1 and R_2:

$$R_1 = \frac{1}{2\pi f_c a_1 C_1}$$
$$R_2 = R_3(A_\infty - 1) \quad \text{and} \quad R_2 = -R_1 A_\infty$$

16.4.2 Second-Order High-Pass Filter

High-pass filters use the same two topologies as the low-pass filters: Sallen−Key and MFB. The only difference is that the positions of the resistors and the capacitors have changed.

16.4.2.1 Sallen−Key Topology

The general Sallen−Key topology in Fig. 16.27 allows for separate gain setting via $A_0 = 1 + R_4/R_3$.
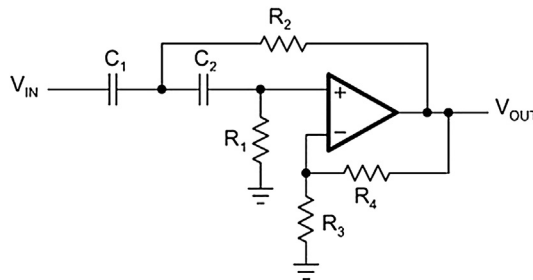
Figure 16.27
General Sallen−Key high-pass filter.
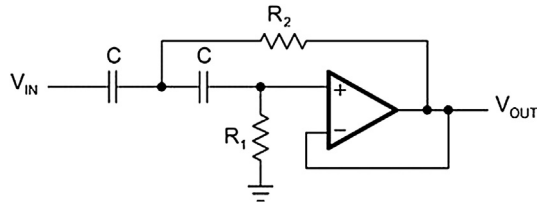
Figure 16.28
Unity-gain Sallen–Key high-pass filter.

The transfer function of the circuit in Fig. 16.27 is given as:

$$A(s) = \frac{\alpha}{1 + \dfrac{R_2(C_1 + C_2) + R_1C_2(1 - \alpha)}{\omega_c R_1 R_2 C_1 C_2} \cdot \dfrac{1}{s} + \dfrac{1}{\omega_c^2 R_1 R_2 C_1 C_2} \cdot \dfrac{1}{s^2}} \qquad \text{with} \quad \alpha = 1 + \frac{R_4}{R_3}$$

The unity-gain topology in Fig. 16.28 is usually applied in low-Q filters with high gain accuracy.

To simplify the circuit design, it is common to choose unity-gain ($\alpha = 1$) and $C_1 = C_2 = C$. The transfer function of the circuit in Fig. 16.28 then simplifies to:

$$A(s) = \frac{1}{1 + \dfrac{2}{\omega_c R_1 C} \cdot \dfrac{1}{s} + \dfrac{2}{\omega_c^2 R_1 R_2 C^2} \cdot \dfrac{1}{s^2}}$$

The coefficient comparison between this transfer function and Eq. (16.5) yields the following:

$$A_\infty = 1$$

$$a_1 = \frac{2}{\omega_c R_1 C}$$

$$b_1 = \frac{1}{\omega_c^2 R_1 R_2 C^2}$$

Given C, the resistor values for R_1 and R_2 are calculated through:

$$R_1 = \frac{1}{\pi f_c C a_1}$$

$$R_2 = \frac{a_1}{4\pi f_c C b_1}$$

16.4.2.2 Multiple Feedback High Pass Filter Topology

To simplify the computation of the circuit, capacitors C_1 and C_3 assume the same value $(C_1 = C_3 = C)$ as shown in Fig. 16.29.

The transfer function of the circuit in Fig. 16.29 is

$$A(s) = \frac{-\dfrac{C}{C_2}}{1 + \dfrac{2C_2 + C}{\omega_c R_1 C_2 C} \cdot \dfrac{1}{s} + \dfrac{2C_2 + C}{\omega_c^2 R_2 R_1 C_2 C} \cdot \dfrac{1}{s^2}}$$

Through coefficient comparison with Eq. (16.5), obtain the following relations:

$$A_\infty = \frac{C}{C_2}$$

$$a_1 = \frac{2C + C_2}{\omega_c R_1 C C_2}$$

$$b_1 = \frac{2C + C_2}{\omega_c R_1 C C_2}$$

Given capacitors C and C_2, and solving for resistors R_1 and R_2:

$$R_1 = \frac{1 - 2A_\infty}{2\pi f_c \cdot C \cdot a_1}$$

$$R_2 = \frac{a_1}{2\pi f_c \cdot b_1 C_2 (1 - 2A_\infty)}$$

The passband gain (A_∞) of an MFB high-pass filter can vary significantly due to the wide tolerances of the two capacitors C and C_2. To keep the gain variation at a minimum, it is necessary to use capacitors with tight tolerance values.
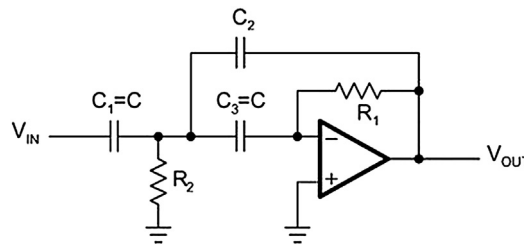
Figure 16.29
Second-order multiple feedback high-pass filter.

16.4.3 Higher-Order High-Pass Filter

Likewise, as with the low-pass filters, higher-order high-pass filters are designed by cascading first-order and second-order filter stages. The filter coefficients are the same ones used for the low-pass filter design and are listed in the coefficient tables (Tables 16.6 through 16.12 in Section 16.9).

Example 16.4. Third Order High-Pass Filter with $f_C = 1$ kHz (Table 16.3).

The task is to design a third-order unity-gain Bessel high-pass filter with the corner frequency $f_C = 1$ kHz. Obtain the coefficients for a third-order Bessel filter from Table 16.6, Section 16.9 and compute each partial filter by specifying the capacitor values and calculating the required resistor values.

16.4.3.1 First Filter

With $C_1 = 100$ nF,

$$R_1 = \frac{1}{2\pi f_c a_1 C_1} = \frac{1}{2\pi \cdot 10^3 \text{ Hz} \cdot 0.756 \cdot 100 \cdot 10^{-9} \text{ F}} = 2.105 \text{ k}\Omega$$

Closest 1% value is 2.1 kΩ.

16.4.3.2 Second Filter

With $C = 100$ nF,

$$R_1 = \frac{1}{\pi f_c C a_1} = \frac{1}{\pi \cdot 10^3 \cdot 100 \cdot 10^{-9} \cdot 0.756} = 3.18 \text{ k}\Omega$$

Closest 1% value is 3.16 kΩ.

$$R_2 = \frac{a_1}{4\pi f_c C b_1} = \frac{0.9996}{4\pi \cdot 10^3 \cdot 100 \cdot 10^{-9} \cdot 0.4772} = 1.67 \text{ k}\Omega$$

Closest 1% value is 1.65 kΩ.

Fig. 16.30 shows the final filter circuit.

Table 16.3 Example 16.4 Filters

	a_i	b_i
Filter 1	$a_1 = 0.756$	$b_1 = 0$
Filter 2	$a_2 = 0.9996$	$b_2 = 0.4772$
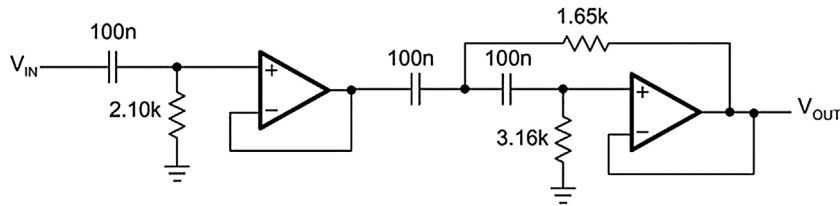
Figure 16.30
Third-order unity-gain Bessel high-pass.

16.5 Band-Pass Filter Design

In Section 16.4, a high-pass response was generated by replacing the term *S* in the low-pass transfer function with the transformation 1/S. Likewise, a band-pass characteristic is generated by replacing the S term with the transformation:

$$\frac{1}{\Delta\Omega}\left(s + \frac{1}{s}\right) \tag{16.7}$$

In this case, the passband characteristic of a low-pass filter is transformed into the upper passband half of a band-pass filter. The upper passband is then mirrored at the mid frequency, f_m ($\Omega = 1$), into the lower passband half (See Fig. 16.31).

The corner frequency of the low-pass filter transforms to the lower and upper -3 dB frequencies of the band-pass, Ω_1 and Ω_2. The difference between both frequencies is defined as the normalized bandwidth $\Delta\Omega$:

$$\Delta\Omega = \Omega_2 - \Omega_1$$
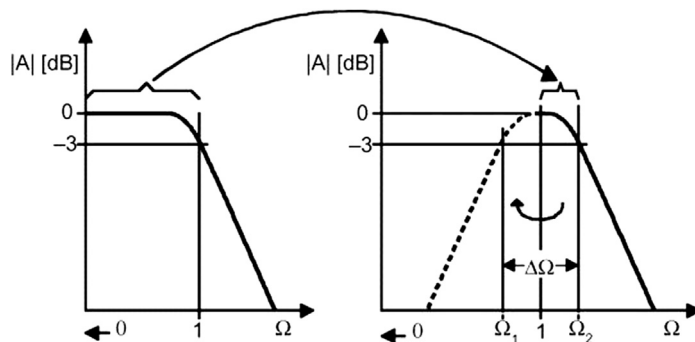
Figure 16.31
Low-pass to band-pass transition.

The normalized mid frequency, where $Q = 1$, is

$$\Omega_m = 1 = \Omega_2 \cdot \Omega_1$$

In analogy to the resonant circuits, the quality factor Q is defined as the ratio of the mid frequency (f_m) to the bandwidth (B):

$$Q = \frac{f_m}{B} = \frac{f_m}{f_2 - f_1} = \frac{1}{\Omega_2 - \Omega_1} = \frac{1}{\Delta\Omega} \qquad (16.8)$$

The simplest design of a band-pass filter is the connection of a high-pass filter and a low-pass filter in series, which is commonly done in wide-band filter applications. Thus, a first-order high-pass and a first-order low-pass provide a second-order band-pass, whereas a second-order high-pass and a second-order low-pass result in a fourth-order band-pass response.

In comparison to wide-band filters, narrow-band filters of higher order consist of cascaded second-order band-pass filters that use the Sallen−Key or the MFB topology.

16.5.1 Second-Order Band-Pass Filter

To develop the frequency response of a second-order band-pass filter, apply the transformation in Eq. (16.7) to a first-order low-pass transfer function:

$$A(s) = \frac{A_0}{1 + s}$$

Replacing s with $\frac{1}{\Delta\Omega}\left(s + \frac{1}{s}\right)$ yields the general transfer function for a second-order band-pass filter:

$$A(s) = \frac{A_0 \cdot \Delta\Omega \cdot s}{1 + \Delta\Omega \cdot s + s^2} \qquad (16.9)$$

When designing band-pass filters, the parameters of interest are the gain at the mid frequency (A_m) and the quality factor (Q), which represents the selectivity of a band-pass filter.

Therefore, replace A_0 with A_m and $\Delta\Omega$ with $1/Q$ (Eq. 16.7) and obtain:

$$A(s) = \frac{\dfrac{A_m}{Q} \cdot s}{1 + \dfrac{1}{Q} \cdot s + s^2} \qquad (16.10)$$

Fig. 16.32 shows the normalized gain response of a second-order band-pass filter for different Qs.

The graph shows that the frequency response of second-order band-pass filters gets steeper with rising Q, thus making the filter more selective.
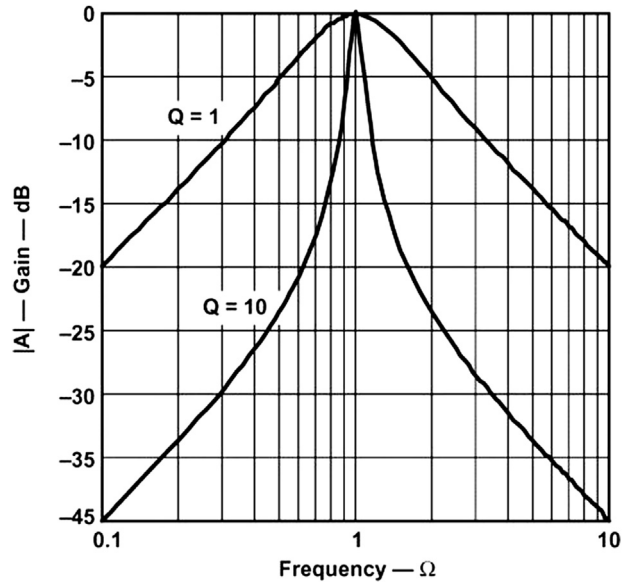
Figure 16.32
Gain response of a second-order band-pass filter.

16.5.1.1 Sallen−Key Topology

The Sallen−Key band-pass circuit in Fig. 16.33 has the following transfer function:

$$A(s) = \frac{G \cdot RC\omega_m \cdot s}{1 + RC\omega_m(3 - G) \cdot s + R^2 C^2 \omega_m^2 \cdot s^2}$$

Through coefficient comparison with Eq. (16.10), obtain the following equations:

$$\text{mid} - \text{frequency}: \quad f_m = \frac{1}{2\pi RC}$$

$$\text{inner gain}: \quad G = 1 + \frac{R_2}{R_1}$$

$$\text{gain at } f_m: \quad A_m = \frac{G}{3 - G}$$

$$\text{filter quality}: \quad Q = \frac{1}{3 - G}$$

The Sallen−Key circuit has the advantage that the quality factor (Q) can be varied via the inner gain (G) without modifying the mid frequency (f_m). A drawback is, however, that Q and A_m cannot be adjusted independently.
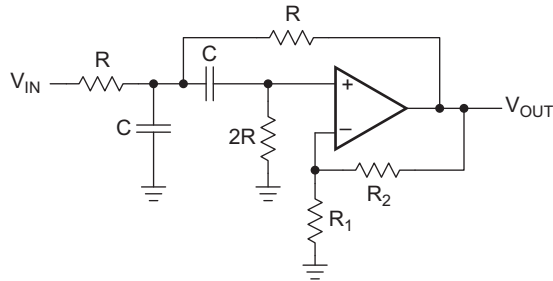
Figure 16.33
Sallen–Key band-pass.

Care must be taken when G approaches the value of 3, because then A_m becomes infinite and causes the circuit to oscillate.

To set the mid frequency of the band-pass, specify f_m and C and then solve for R:

$$R = \frac{1}{2\pi f_m C}$$

Because of the dependency between Q and A_m, there are two options to solve for R_2; either to set the gain at mid frequency:

$$R_2 = \frac{2A_m - 1}{1 + A_m}$$

or to design for a specified Q:

$$R_2 = \frac{2Q - 1}{Q}$$

16.5.1.2 Multiple Feedback Band Pass Filter Topology

The MFB band-pass circuit in Fig. 16.34 has the following transfer function:

$$A(s) = \frac{-\dfrac{R_2 R_3}{R_1 + R_3} C\omega_m \cdot s}{1 + \dfrac{2R_1 R_3}{R_1 + R_3} C\omega \cdot s + \dfrac{R_1 R_2 R_3}{R_1 + R_3} C^2 \cdot \omega_m^2 \cdot s^2}$$
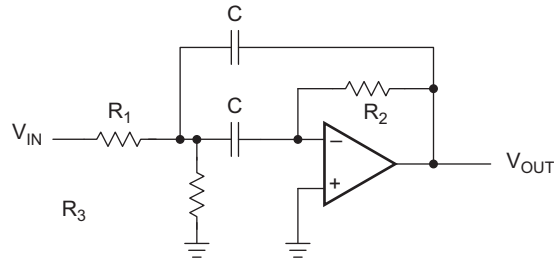
Figure 16.34
Multiple feedback band-pass.

The coefficient comparison with Eq. (16.9), yields the following equations:

$$\text{mid} - \text{frequency}: \quad f_m = \frac{1}{1\pi C}\sqrt{\frac{R_1 + R_3}{R_1 R_2 R_3}}$$

$$\text{gain at } f_m: \quad -A_m = \frac{R_2}{2R_1}$$

$$\text{filter quality}: \quad Q = \pi f_m R_2 C$$

$$\text{bandwidth}: \quad B = \frac{1}{\pi R_2 C}$$

The MFB band-pass allows to adjust Q, A_m, and fm independently. Bandwidth and gain factor do not depend on R_3. Therefore, R_3 can be used to modify the mid frequency without affecting bandwidth, B, or gain, A_m. For low values of Q, the filter can work without R_3; however, Q then depends on A_m via:

$$-A_m = 2Q^2$$

Example 16.5. Second-Order MFB Band-Pass Filter with f_m = 1 kHz.

To design a second-order MFB band-pass filter with a mid frequency of $f_m = 1$ kHz, a quality factor of Q = 10, and a gain of $A_m = -2$, assume a capacitor value of C = 100 nF, and solve the previous equations for R_1 through R_3 in the following sequence:

$$R_2 = \frac{Q}{\pi f_m C} = \frac{10}{\pi \cdot 1 \text{ kHz} \cdot 100 \text{ nF}} = 31.8 \text{ k}\Omega$$

$$R_1 = \frac{R_2}{-2A_m} = \frac{31.8 \text{ k}\Omega}{4} = 7.96 \text{ k}\Omega$$

$$R_3 = \frac{-A_m R_1}{2Q^2 + A_m} = \frac{2 \cdot 7.96 \text{ k}\Omega}{200 - 2} = 80.4 \text{ }\Omega$$

16.5.2 Fourth-Order Band-Pass Filter (Staggered Tuning)

Fig. 16.32 shows that the frequency response of second-order band-pass filters gets steeper with rising Q. However, there are band-pass applications that require a flat gain response close to the mid frequency as well as a sharp passband-to-stopband transition. These tasks can be accomplished by higher-order band-pass filters.

Of particular interest is the application of the low-pass to band-pass transformation onto a second-order low-pass filter, since it leads to a fourth-order band-pass filter.

Replacing the S term in Eq. (16.2) with Eq. (16.7) gives the general transfer function of a fourth-order band-pass:

$$A(s) = \frac{\dfrac{s^2 \cdot A_0 (\Delta\Omega)^2}{b_1}}{1 + \dfrac{a_1}{b_1}\Delta\Omega \cdot s + \left[2 + \dfrac{(\Delta\Omega)^2}{b_1}\right] \cdot s^2 + \dfrac{a_1}{b_1}\Delta\Omega \cdot s^3 + s^4} \qquad (16.11)$$

Similar to the low-pass filters, the fourth-order transfer function is split into two second-order band-pass terms. Further mathematical modifications yield:

$$A(s) = \frac{\dfrac{A_{mi}}{Q_i} \cdot \alpha s}{\left[1 + \dfrac{\alpha s}{Q_1} + (\alpha s)^2\right]} \cdot \frac{\dfrac{A_{mi}}{Q_i}\dfrac{s}{\alpha}}{\left[1 + \dfrac{1}{Q_i}\left(\dfrac{s}{\alpha}\right) + \left(\dfrac{s}{\alpha}\right)^2\right]} \qquad (16.12)$$

Eq. (16.12) represents the connection of two second-order band-pass filters in series, where

- A_{mi} is the gain at the mid frequency, f_{mi}, of each partial filter,
- Q_i is the pole quality of each filter, and
  - α and $1/\alpha$ are the factors by which the mid frequencies of the individual filters, f_{m1} and f_{m2}, derive from the mid frequency, f_m, of the overall bandpass.

In a fourth-order band-pass filter with high Q, the mid frequencies of the two partial filters differ only slightly from the overall mid frequency. This method is called staggered tuning.

Factor α needs to be determined through successive approximation, using Eqs. (16)−(13):

$$\alpha^2 + \left[\frac{\alpha \cdot \Delta\Omega \cdot a_1}{b_1(1 + \alpha^2)}\right]^2 + \frac{1}{\alpha^2} - 2 - \frac{(\Delta\Omega)^2}{b_1} = 0 \qquad (16.13)$$

with a_1 and b_1 being the second-order low-pass coefficients of the desired filter type.

To simplify the filter design, Table 16.4 lists those coefficients and provides the α values for three different quality factors, $Q = 1$, $Q = 10$, and $Q = 100$.

Table 16.4: Values of α for Different Filter Types

	Bessel				Butterworth				Tschebyscheff		
a_1	1.3617			a_1	1.4142			a_1	1.0650		
b_1	0.6180			b_1	1.0000			b_1	1.9305		
Q	100	10	1	Q	100	10	1	Q	100	10	1
$\Delta\Omega$	0.01	0.1	1	$\Delta\Omega$	0.01	0.1	1	$\Delta\Omega$	0.01	0.1	1
α	1.0032	1.0324	1.438	α	1.0035	1.036	1.4426	α	1.0033	1.0338	1.39

After α has been determined, all quantities of the partial filters can be calculated using the following equations:

The mid frequency of filter 1 is

$$f_{m1} = \frac{f_m}{\alpha} \tag{16.14}$$

the mid frequency of filter 2 is

$$f_{m2} = f_m \cdot \alpha \tag{16.15}$$

with f_m being the mid frequency of the overall forth-order band-pass filter.

The individual pole quality, Q_i, is the same for both filters:

$$Q_i = Q \cdot \frac{(1 + \alpha^2) b_1}{\alpha \cdot a_1} \tag{16.16}$$

with Q being the quality factor of the overall filter.

The individual gain (A_{mi}) at the partial mid frequencies, f_{m1} and f_{m2}, is the same for both filters:

$$A_{mi} = \frac{Q_i}{Q} \cdot \sqrt{\frac{A_m}{B_1}} \tag{16.17}$$

with A_m being the gain at mid frequency, f_m, of the overall filter.

Example 16.6. Fourth-Order Butterworth Band-Pass Filter.

The task is to design a fourth-order Butterworth band-pass with the following parameters:

- mid frequency, $f_m = 10$ kHz,
- bandwidth, $B = 1000$ Hz, and
- and gain, $A_m = 1$.

From Table 16.4 the following values are obtained:

- $a_1 = 1.4142$,
- $b_1 = 1$, and
- $\alpha = 1.036$.

In accordance with Eqs. (16.14) and (16.15), the mid frequencies for the partial filters are

$$f_{mi} = \frac{10 \text{ kHz}}{1.036} = 9.653 \text{ kHz} \quad \text{and} \quad f_{m2} = 10 \text{ kHz} \cdot 1.036 = 10.36 \text{ kHz}$$

The overall Q is defined as $Q = f_m/B$, and for this example results in $Q = 10$.

Using Eq. (16.16), the Q_i of both filters is

$$Q_i = 10 \cdot \frac{(1 + 1.036^2) \cdot 1}{1.036 \cdot 1.4142} = 14.15$$

With Eq. (16.17), the passband gain of the partial filters at f_{m1} and f_{m2} calculates to:

$$A_{mi} = \frac{14.15}{10} \cdot \sqrt{\frac{1}{1}} = 1.415$$

Eqs. (16.16) and (16.17) show that Q_i and A_{mi} of the partial filters need to be independently adjusted. The only circuit that accomplishes this task is the MFB band-pass filter in Section 16.5.1.2.

To design the individual second-order band-pass filters, specify $C = 10$ nF, and insert the previously determined quantities for the partial filters into the resistor equations of the MFB band-pass filter. The resistor values for both partial filters are calculated below.

Filter 1 :

$$R_{21} = \frac{Q_i}{\pi f_{m1} C} = \frac{14.15}{\pi \cdot 9.653 \text{ kHz} \cdot 10 \text{ nF}} = 46.7 \text{ k}\Omega$$

$$R_{11} = \frac{R_{21}}{-2A_{mi}} = \frac{46.7 \text{ k}\Omega}{-2 \cdot -1.415} = 16.5 \text{ k}\Omega$$

$$R_{31} = \frac{-A_{mi}R_{11}}{2Q_i^2 + A_{mi}} = \frac{1.415 \cdot 16.5 \text{ k}\Omega}{2 \cdot 14.15^2 + 1.415} = 58.1 \text{ }\Omega$$

Filter 2 :

$$R_{22} = \frac{Q_i}{\pi f_{m2} C} = \frac{14.15}{\pi \cdot 10.36 \text{ kHz} \cdot 10 \text{ nF}} = 43.5 \text{ k}\Omega$$

$$R_{12} = \frac{R_{22}}{-2A_{mi}} = \frac{43.5}{-2 \cdot -1.415} = 15.4 \text{ k}\Omega$$

$$R_{32} = \frac{A_{mi}R_{12}}{2Q_i^2 + A_{mi}} = \frac{1.415 \cdot 15.4 \text{ k}\Omega}{2 \cdot 14.15^2 + 1.415} = 54.2 \text{ }\Omega$$

Fig. 16.35 compares the gain response of a fourth-order Butterworth band-pass filter with $Q = 1$ and its partial filters to the fourth-order gain of Example 16.4 with $Q = 10$.
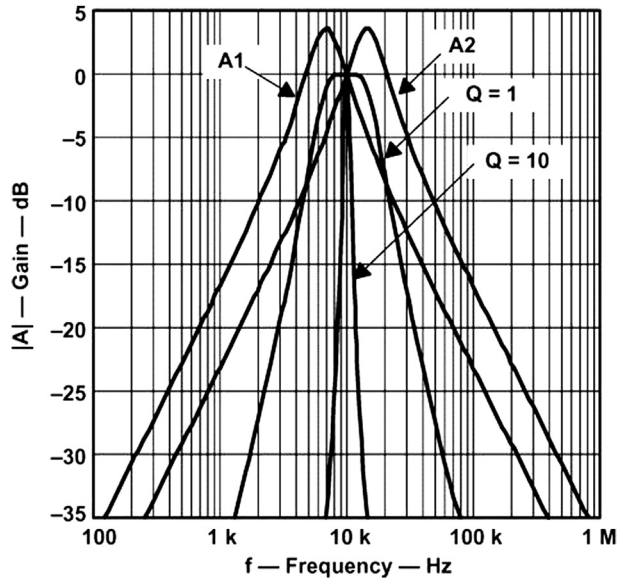
Figure 16.35
Gain responses of a fourth-order Butterworth band-pass and its partial filters.

16.6 Band-Rejection Filter Design

A band-rejection filter is used to suppress a certain frequency rather than a range of frequencies.

Two of the most popular band-rejection filters are the active twin-T and the active Wien-Robinson circuit, both of which are second-order filters.

To generate the transfer function of a second-order band-rejection filter, replace the s term of a first-order low-pass response with the transformation in Eq. (16.18):

$$\frac{\Delta\Omega}{s + \dfrac{1}{s}} \tag{16.18}$$

which gives

$$A(s) = \frac{A_0\left(1 + s^2\right)}{1 + \Delta\Omega \cdot s + s^2} \tag{16.19}$$

Thus the passband characteristic of the low-pass filter is transformed into the lower passband of the band-rejection filter. The lower passband is then mirrored at the mid frequency, f_m ($\Omega = 1$), into the upper passband half (Fig. 16.36).
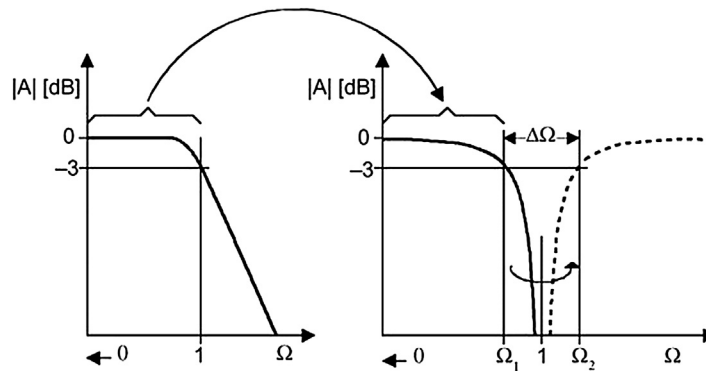
Figure 16.36
Low-pass to band-rejection transition.

The corner frequency of the low-pass transforms to the lower and upper -3-dB frequencies of the band-rejection filter Ω_1 and Ω_2. The difference between both frequencies is the normalized bandwidth $\Delta\Omega$:

$$\Delta\Omega = \Omega_{\max} - \Omega_{\min}$$

Identical to the selectivity of a band-pass filter, the quality of the filter rejection is defined as:

$$Q = \frac{f_m}{B} = \frac{1}{\Delta\Omega}$$

Therefore, replacing $\Delta\Omega$ in Eq. (16.19) with $1/Q$ yields:

$$A(s) = \frac{A_0(1 + s^2)}{1 + \dfrac{1}{Q}\cdot s + s^2} \tag{16.20}$$

16.6.1 Active Twin-T Filter

The original twin-T filter, shown in Fig. 16.37, is a passive RC-network with a quality factor of $Q = 0.25$. To increase Q, the passive filter is implemented into the feedback loop of an amplifier, thus turning into an active band-rejection filter, shown in Fig. 16.38.

The transfer function of the active twin-T filter is

$$A(s) = \frac{k(1 + s^2)}{1 + 2(2 - k)\cdot s + s^2} \tag{16.21}$$
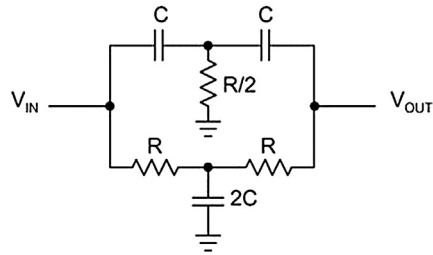
Figure 16.37
Passive Twin-T filter.
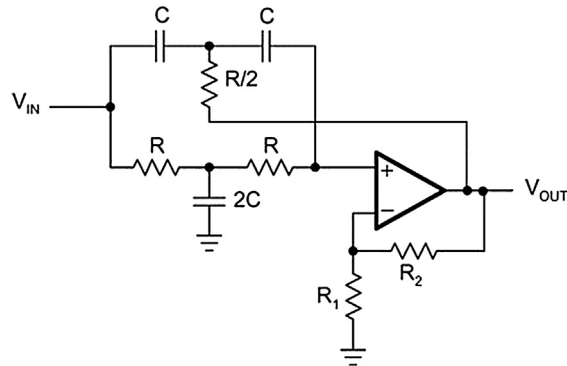
Figure 16.38
Active Twin-T filter.

Comparing the variables of Eq. (16.21) with Eq. (16.20) provides the equations that determine the filter parameters:

$$\text{mid} - \text{frequency}: \quad f_m = \frac{1}{2\pi RC}$$

$$\text{inner gain}: \quad G = 1 + \frac{R_2}{R_1}$$

$$\text{passband gain}: \quad A_0 = G$$

$$\text{rejection quality}: \quad Q = \frac{1}{2(2 - G)}$$

The twin-T circuit has the advantage that the quality factor (Q) can be varied via the inner gain (G) without modifying the mid frequency (f_m). However, Q and Am cannot be adjusted independently.

To set the mid frequency of the band-pass, specify f_m and C, and then solve for R:

$$R = \frac{1}{2\pi f_m C}$$

Because of the dependency between Q and A_m, there are two options to solve for R_2; either to set the gain at mid frequency:

$$R_2 = (A_0 - 1)R_1$$

or to design for a specific Q:

$$R_2 = R_1\left(1 - \frac{1}{2Q}\right)$$

16.6.2 Active Wien-Robinson Filter

The Wien-Robinson bridge in Fig. 16.39 is a passive band-rejection filter with differential output. The output voltage is the difference between the potential of a constant voltage divider and the output of a band-pass filter. Its Q-factor is close to that of the twin-T circuit. To achieve higher values of Q, the filter is connected into the feedback loop of an amplifier.

The active Wien-Robinson filter in Fig. 16.40 has the transfer function:

$$A(s) = -\frac{\dfrac{\beta}{1+\alpha}(1+s^2)}{1 + \dfrac{3}{1+\alpha}\cdot s + s^2} \tag{16.22}$$

with $\alpha = \dfrac{R_2}{R_3}$ and $\beta = \dfrac{R_2}{R_4}$
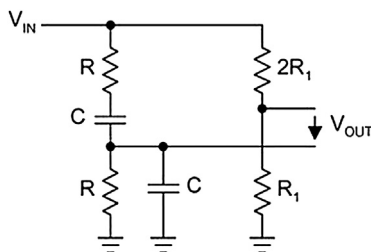
Figure 16.39
Passive Wien-Robinson bridge.
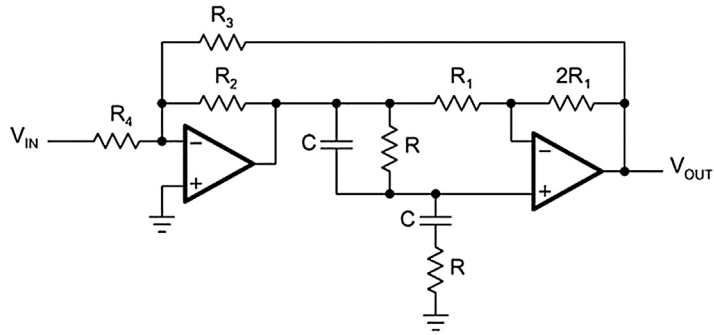
Figure 16.40
Active Wien-Robinson filter.

Comparing the variables of Eq. (16.22) with Eq. (16.20) provides the equations that determine the filter parameters:

$$\text{mid} - \text{frequency}: \quad f_m = \frac{1}{2\pi RC}$$

$$\text{passband gain}: \quad A_0 = -\frac{\beta}{1 + \alpha}$$

$$\text{rejection quality}: \quad Q = \frac{1 + \alpha}{3}$$

To calculate the individual component values, establish the following design procedure:

1. Define f_m and C and calculate R with:

$$R = \frac{1}{2\pi f_m C}$$

2. Specify Q and determine α via:

$$\alpha = 3Q - 1$$

3. Specify A_0 and determine β via:

$$\beta = -A_0 \cdot 3Q$$

4. Define R_2 and calculate R_3 and R_4 with:

$$R_3 = \frac{R_2}{\alpha}$$
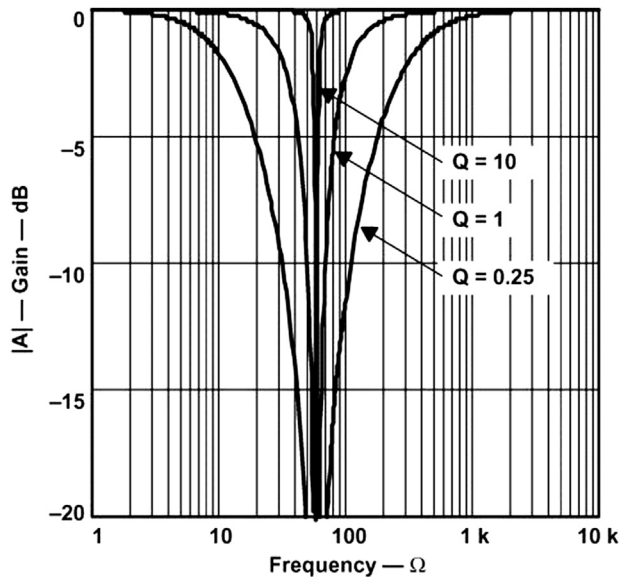
Figure 16.41
Comparison of Q between passive and active band-rejection filters.

and

$$R_4 = \frac{R_2}{\beta}$$

In comparison to the twin-T circuit, the Wien-Robinson filter allows modification of the passband gain, A_0, without affecting the quality factor, Q.

If fm is not completely suppressed due to component tolerances of R and C, a fine-tuning of the resistor $2R_2$ is required.

Fig. 16.41 shows a comparison between the filter response of a passive band-rejection filter with $Q = 0.25$ and an active second-order filter with $Q = 1$ and $Q = 10$.

16.7 All-Pass Filter Design

In comparison to the previously discussed filters, an all-pass filter has a constant gain across the entire frequency range, and a phase response that changes linearly with frequency.

Because of these properties, all-pass filters are used in phase compensation and signal delay circuits.

Similar to the low-pass filters, all-pass circuits of higher order consist of cascaded first-order and second-order all-pass stages. To develop the all-pass transfer function from a low-pass response, replace A_0 with the conjugate complex denominator.

The general transfer function of an all-pass is

$$A(s) = \frac{\prod_i (1 - a_i s + b_i s^2)}{\prod_i (1 + a_i s + b_i s^2)} \tag{16.23}$$

with a_i and b_i being the coefficients of a partial filter. The all-pass coefficients are listed in Table 16.12 of Section 16.9.

Expressing Eq. (16.23) in magnitude and phase yields

$$A(s) = \frac{\prod_i \sqrt{\left(1 - b_i \Omega^2\right)^2 + a_i^2 \Omega^2} \cdot e^{-ja}}{\prod_i \sqrt{\left(1 - b_i \Omega^2\right)^2 + a_i^2 \Omega^2} \cdot e^{+ja}} \tag{16.24}$$

This gives a constant gain of 1, and a phase shift, φ, of:

$$\varphi = -2\alpha = -2 \sum_i \arctan \frac{a_i \Omega}{1 - b_i \Omega^2} \tag{16.25}$$

To transmit a signal with minimum phase distortion, the all-pass filter must have a constant group delay across the specified frequency band. The group delay is the time by which the all-pass filter delays each frequency within that band.

The frequency at which the group delay drops to $1/\sqrt{2}$ times its initial value is the corner frequency, f_C.

The group delay is defined through:

$$t_{gr} = -\frac{d\varphi}{d\omega} \tag{16.26}$$

To present the group delay in normalized form, refer t_{gr} to the period of the corner frequency, T_C, of the all-pass circuit:

$$T_{gr} = \frac{t_{gr}}{T_c} = t_{gr} \cdot f_c = t_{gr} \cdot \frac{\omega_c}{2\pi} \tag{16.27}$$

Substituting t_{gr} through Eq. (16.26) gives

$$T_{gr} = -\frac{1}{2\pi} \cdot \frac{d\varphi}{d\Omega}$$

(16.28)

Inserting the φ term in Eq. (16.25) into Eq. (16.28) and completing the derivation, results in:

$$T_{gr} = \frac{1}{\pi} \sum_i \frac{a_i \left(1 + b_i \Omega^2\right)}{1 + \left(a_i^2 - 2b_1\right) \cdot \Omega^2 + b_1^2 \Omega^4}$$

(16.29)

Setting $\Omega = 0$ in Eq. (16.29) gives the group delay for the low frequencies, $0 < \Omega < 1$, which is

$$T_{gr0} = \frac{1}{\pi} \sum_i a_i$$

(16.30)

The values for T_{gr0} are listed in Table 16.12, Section 16.9, from the first to the tenth order.

In addition, Fig. 16.42 shows the group delay response versus the frequency for the first ten orders of all-pass filters.
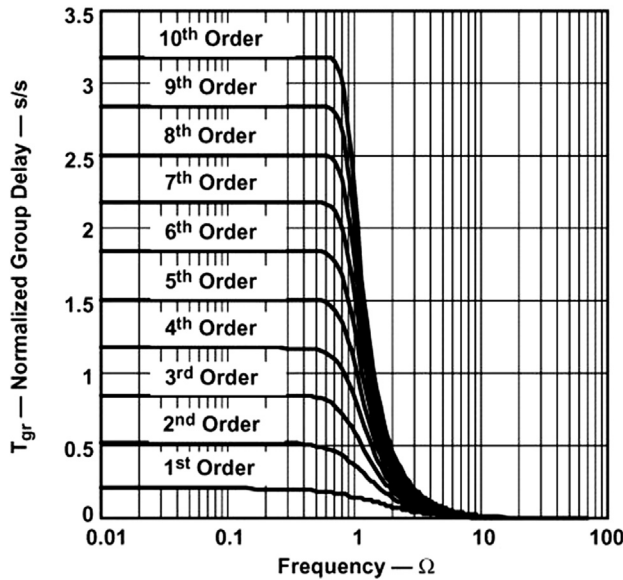
Figure 16.42
Frequency response of the group delay for the first 10 filter orders.

16.7.1 First-Order All-Pass Filter

Fig. 16.43 shows a first-order all-pass filter with a gain of $+1$ at low frequencies and a gain of -1 at high frequencies. Therefore, the magnitude of the gain is 1, while the phase changes from 0 degrees to -180 degrees.

The transfer function of the circuit above is

$$A(s) = \frac{1 - RC\omega_c \cdot s}{1 + RC\omega_c \cdot s}$$

The coefficient comparison with Eq. (16.23) ($b1 = 1$) results in:

$$a_i = RC \cdot 2\pi f_c \qquad\qquad (16.31)$$

To design a first-order all-pass, specify f_C and C and then solve for R:

$$R = \frac{a_i}{2\pi f_c \cdot C} \qquad\qquad (16.32)$$

Inserting Eq. (16.31) into Eq. (16.30) and substituting ω_C with Eq. (16.27) provides the maximum group delay of a first-order all-pass filter:

$$t_{gr0} = 2RC \qquad\qquad (16.33)$$

16.7.2 Second-Order All-Pass Filter

Fig. 16.44 shows that one possible design for a second-order all-pass filter is to subtract the output voltage of a second-order band-pass filter from its input voltage.

The transfer function of the circuit in Fig. 16.44 is

$$A(s) = \frac{1 + (2R_1 - \alpha R_2)C\omega_c \times s + R_1 R_2 C^2 \omega_c^2 \times s^2}{1 + 2R_1 C\omega_c \times s + R_1 R_2 C^2 \omega_c^2 \times s^2}$$
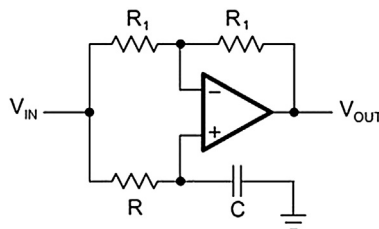
Figure 16.43
First-order all-pass.
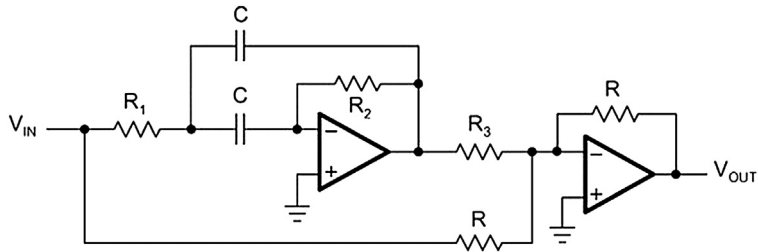
Figure 16.44
Second-order all-pass filter.

The coefficient comparison with Eq. (16.23) yields

$$a_1 = 4\pi f_c R_1 C \qquad (16.34)$$

$$b_1 = a_1 \pi f_c R_2 C \qquad (16.35)$$

$$\alpha = \frac{a_1^2}{b_1} = \frac{R}{R_3} \qquad (16.36)$$

To design the circuit, specify f_C, C, and R, and then solve for the resistor values:

$$R_1 = \frac{a_1}{4\pi f_c C} \qquad (16.37)$$

$$R_2 = \frac{b_1}{a_1 \pi f_c C} \qquad (16.38)$$

$$R_3 = \frac{R}{\alpha} \qquad (16.39)$$

Inserting Eq. (16.34) into Eq. (16.30) and substituting ω_C with Eq. (16.27) gives the maximum group delay of a second-order all-pass filter:

$$t_{gr0} = 4R_1 C \qquad (16.40)$$

16.7.3 Higher-Order All-Pass Filter

Higher-order all-pass filters consist of cascaded first-order and second-order filter stages.

Example 16.7. 2-ms Delay All-Pass Filter.

A signal with the frequency spectrum, $0 < f < 1$ kHz, needs to be delayed by 2 ms. To keep the phase distortions at a minimum, the corner frequency of the all-pass filter must be $f_C \geq 1$ kHz.

Eq. (16.27) determines the normalized group delay for frequencies below 1 kHz:

$$T_{gr0} = \frac{t_{gr0}}{T_c} = 2 \text{ ms} \cdot 1 \text{ kHz} = 2.0$$

Fig. 16.42 confirms that a seventh-order all-pass is needed to accomplish the desired delay. The exact value, however, is $T_{gr0} = 2.1737$. To set the group delay to precisely 2 ms, solve Eq. (16.27) for f_C and obtain the corner frequency:

$$f_C = \frac{T_{gr0}}{t_{gr0}} = 1.087 \text{ kHz}$$

To complete the design, look up the filter coefficients for a seventh-order all-pass filter, specify C, and calculate the resistor values for each partial filter.

Cascading the first-order all-pass with the three second-order stages results in the desired seventh-order all-pass filter (See Fig. 16.45).

16.8 Practical Design Hints

This section introduces DC-biasing techniques for filter designs in single-supply applications, which are usually not required when operating with dual supplies. It also provides recommendations on selecting the type and value range of capacitors and resistors as well as the decision criteria for choosing the correct op amp.

16.8.1 Filter Circuit Biasing

The filter diagrams in this chapter are drawn for dual supply applications. The op amp operates from a positive and a negative supply, while the input and the output voltage are referenced to ground (Fig. 16.46).

For the single supply circuit in Fig. 16.47, the lowest supply voltage is ground. For a symmetrical output signal, the potential of the noninverting input is level-shifted to midrail.

The coupling capacitor, C_{IN} in Fig. 16.47, AC-couples the filter, blocking any unknown DC level in the signal source. The voltage divider, consisting of the two equal-bias resistors R_B, divides the supply voltage to V_{MID} and applies it to the inverting op amp input.

For simple filter input structures, passive RC networks often provide a low-cost biasing solution. In the case of more complex input structures, such as the input of a second-order low-pass filter, the RC network can affect the filter characteristic. Then it is necessary to
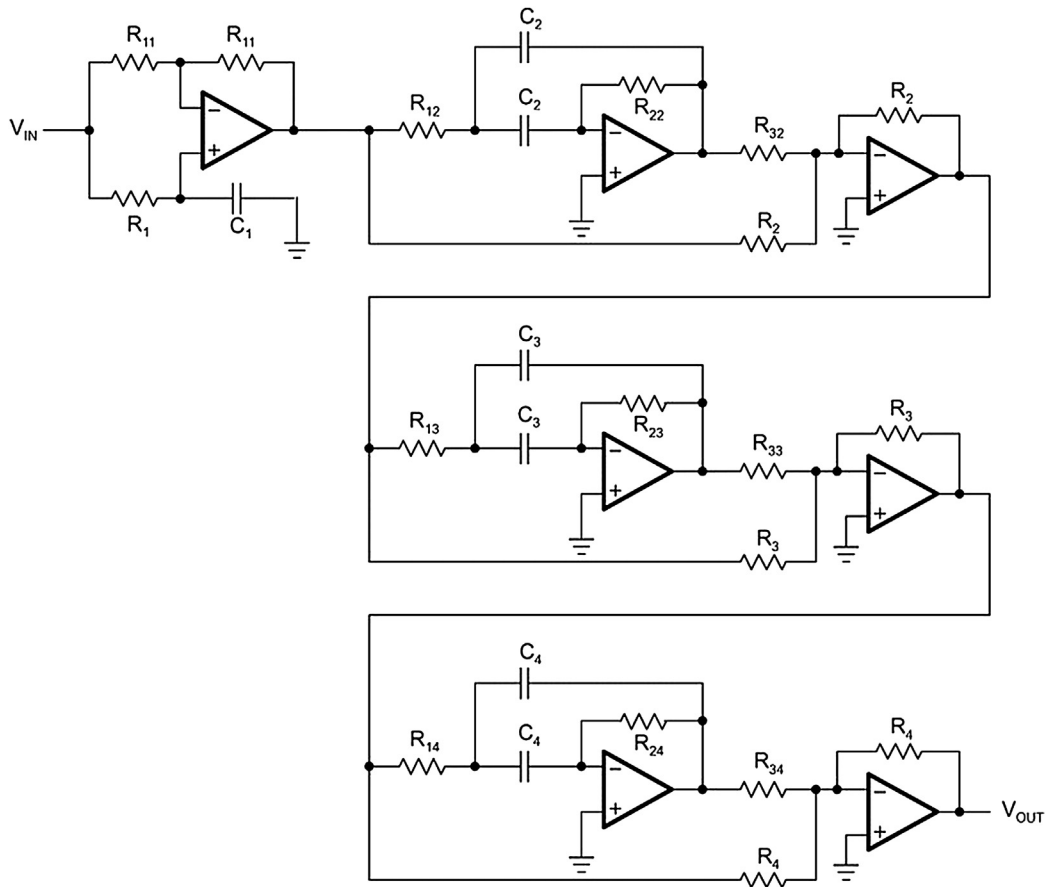
Figure 16.45
Seventh-order all-pass filter.
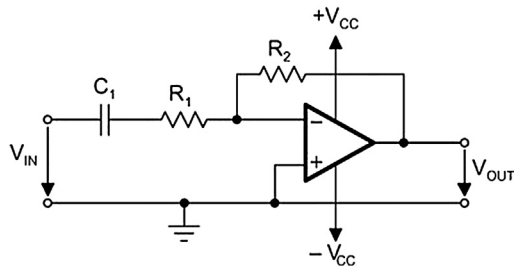
Figure 16.46
Dual-supply filter circuit.
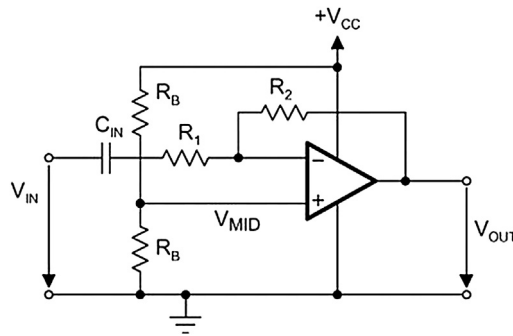
Figure 16.47
Single-supply filter circuit.
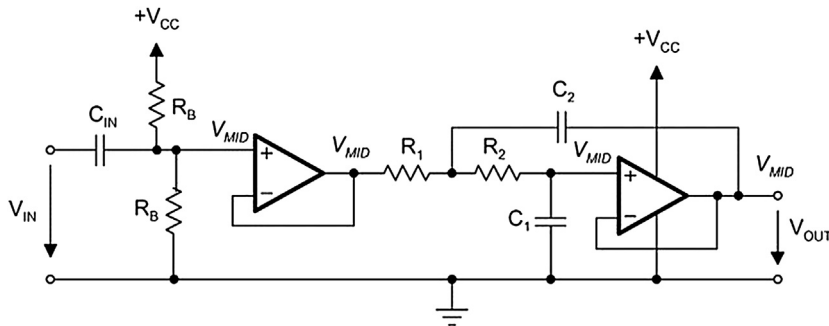
Figure 16.48
Biasing a Sallen–Key low-pass.

either include the biasing network into the filter calculations or to insert an input buffer between biasing network and the actual filter circuit, as shown in Fig. 16.48.

C_{IN} AC-couples the filter, blocking any DC level in the signal source. V_{MID} is derived from V_{CC} via the voltage divider. The op amp operates as a voltage follower and as an impedance converter. V_{MID} is applied via the DC path, R_1 and R_2, to the noninverting input of the filter amplifier.

Note that the parallel circuit of the resistors, R_B, together with C_{IN} creates a high-pass filter. To avoid any effect on the low-pass characteristic, the corner frequency of the input high-pass must be low versus the corner frequency of the actual low-pass.

The use of an input buffer causes no loading effects on the low-pass filter, thus keeping the filter calculation simple.
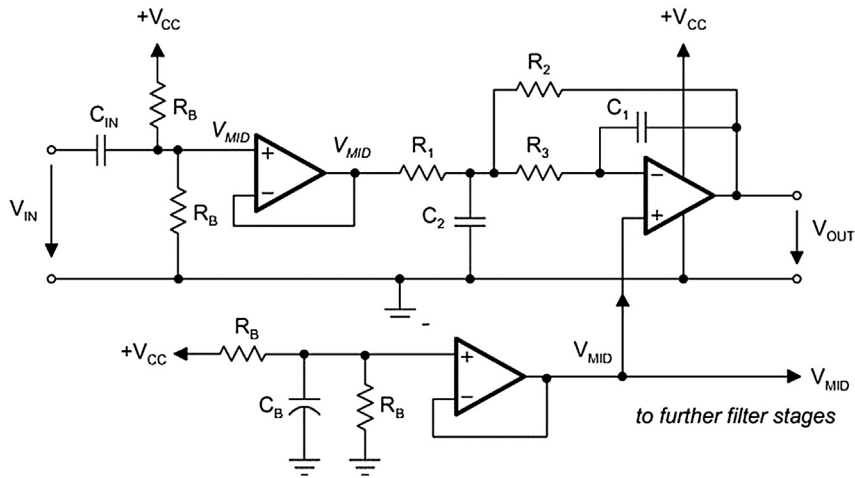
Figure 16.49
Biasing a second-order multiple feedback low-pass filter.

In the case of a higher-order filter, all following filter stages receive their bias level from the preceding filter amplifier.

Fig. 16.49 shows the biasing of an MFB low-pass filter.

The input buffer decouples the filter from the signal source. The filter itself is biased via the noninverting amplifier input. For that purpose, the bias voltage is taken from the output of a V_{MID} generator with low output impedance. The op amp operates as a difference amplifier and subtracts the bias voltage of the input buffer from the bias voltage of the V_{MID} generator, thus yielding a DC potential of V_{MID} at zero input signal.

A low-cost alternative is to remove the op amp and to use a passive biasing network instead. However, to keep loading effects at a minimum, the values for R_B must be significantly higher than without the op amp.

The biasing of a Sallen−Key and an MFB high-pass filter is shown in Fig. 16.50.

The input capacitors of high-pass filters already provide the AC-coupling between filter and signal source. Both circuits use the V_{MID} generator from Fig. 16.50 for biasing. While the MFB circuit is biased at the noninverting amplifier input, the Sallen−Key high-pass is biased via the only DC path available, which is R_1. In the AC circuit, the input signals travel via the low output impedance of the op amp to ground.

16.8.2 Capacitor Selection

The tolerance of the selected capacitors and resistors depends on the filter sensitivity and on the filter performance.
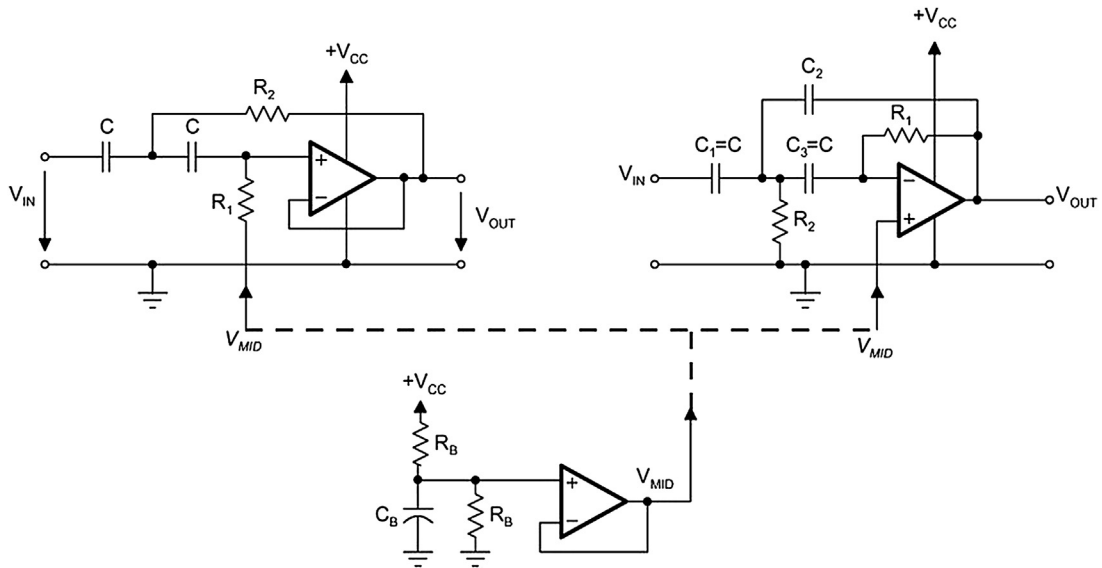
Figure 16.50
Biasing a Sallen–Key and a multiple feedback high-pass filter.

Sensitivity is the measure of the vulnerability of a filter's performance to changes in component values. The important filter parameters to consider are the corner frequency, f_C, and Q.

For example, when Q changes by $\pm 2\%$ due to a $\pm 5\%$ change in the capacitance value, then the sensitivity of Q to capacity changes is expressed as: $s\frac{Q}{C} = \frac{2\%}{5\%} = 0.4\frac{\%}{\%}$. The following sensitivity approximations apply to second-order Sallen–Key and MFB filters:

$$s\frac{Q}{C} \approx s\frac{Q}{C} \approx s\frac{f_c}{C} \approx \pm \ 0.5\frac{\%}{\%}$$

Although 0.5%/% is a small difference from the ideal parameter, in the case of higher-order filters, the combination of small Q and f_C differences in each partial filter can significantly modify the overall filter response from its intended characteristic.

Figs. 16.51 and 16.52 show how an intended eighth-order Butterworth low-pass can turn into a low-pass with Tschebyscheff characteristic mainly due to capacitance changes from the partial filters.

Fig. 16.51 shows the differences between the ideal and the actual frequency responses of the four partial filters. The overall filter responses are shown in Fig. 16.52. The difference between ideal and real response peaks with 0.35 dB at approximately 30 kHz, which is equivalent to an enormous 4.1% gain error can be seen.
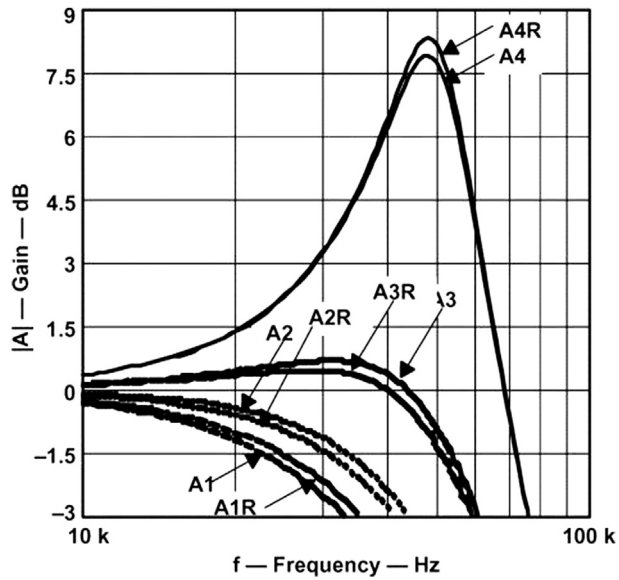
Figure 16.51
Differences in Q and f_C in the partial filters of an eighth-order Butterworth low-pass filter.
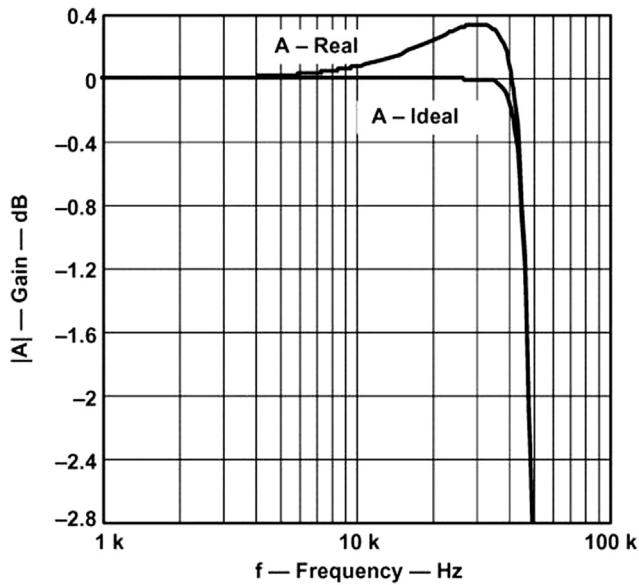
Figure 16.52
Modification of the intended Butterworth response to a Tschebyscheff-type characteristic.

If this filter is intended for a data acquisition application, it could be used at best in a 4-bit system. In comparison, if the maximum full-scale error of a 12-bit system is given with ½ LSB, then maximum pass-band deviation would be −0.001 dB, or 0.012%.

To minimize the variations of f_C and Q, NPO (COG) ceramic capacitors are recommended for high-performance filters. These capacitors hold their nominal value over a wide temperature and voltage range. The various temperature characteristics of ceramic capacitors are identified by a three-symbol code such as: COG, X7R, Z5U, and Y5V.

COG-type ceramic capacitors are the most precise. Their nominal values range from 0.5 pF to approximately 47 nF with initial tolerances from ±0.25 pF for smaller values and up to ±1% for higher values. Their capacitance drift over temperature is typically 30 ppm/°C.

X7R-type ceramic capacitors range from 100 pF to 2.2 μF with an initial tolerance of +1% and a capacitance drift over temperature of ±15%.

For higher values, tantalum electrolytic capacitors should be used.

Other precision capacitors are silver mica, metallized polycarbonate, and for high temperatures, polypropylene or polystyrene.

Since capacitor values are not as finely subdivided as resistor values, the capacitor values should be defined prior to selecting resistors. If precision capacitors are not available to provide an accurate filter response, then it is necessary to measure the individual capacitor values and to calculate the resistors accordingly.

For high performance filters, 0.1% resistors are recommended.

16.8.3 Component Values

Resistor values should stay within the range of 1—100 kΩ. The lower limit avoids excessive current draw from the op amp output, which is particularly important for single-supply op amps in power-sensitive applications. Those amplifiers have typical output currents of between 1 mA and 5 mA. At a supply voltage of 5 V, this current translates to a minimum of 1 kΩ.

The upper limit of 100 kΩ is to avoid excessive resistor noise.

Capacitor values can range from 1 nF to several μF. The lower limit avoids coming too close to parasitic capacitances. If the common-mode input capacitance of the op amp, used in a Sallen—Key filter section, is close to 0.25% of C_1, ($C_1/400$), it must be considered for

accurate filter response. The MFB topology, in comparison, does not require input-capacitance compensation.

16.8.4 Op Amp Selection

The most important op amp parameter for proper filter functionality is the unity-gain bandwidth. In general, the open-loop gain (AOL) should be 100 times (40 dB above) the peak gain (Q) of a filter section to allow a maximum gain error of 1% (See Fig. 16.53).

The following equations are good rules of thumb to determine the necessary unity-gain bandwidth of an op amp for an individual filter section.

1. First-order filter:

$$f_T = 100 \cdot Gain \cdot f_c$$

2. Second-order filter (Q < 1):

$$f_T = 100 \cdot Gain \cdot f_c \cdot k_i \quad with \quad k_i = \frac{f_{ci}}{f_c}$$

3. Second-order filter (Q > 1):

$$f_T = 100 \cdot Gain \cdot \frac{f_C}{a_i} \sqrt{\frac{Q_i^2 - 0.5}{Q_i^2 - 0.25}}$$
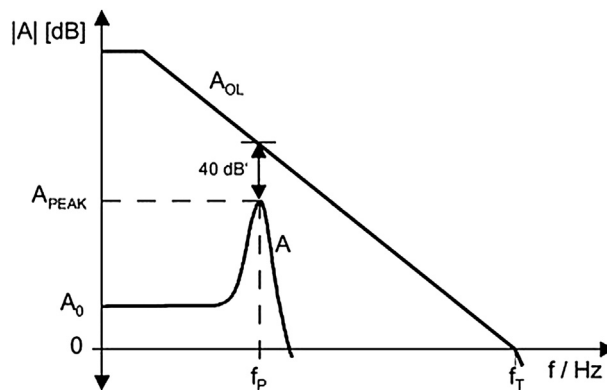
Figure 16.53
Open-loop gain (A$_{OL}$) and filter response (A).

For example, a fifth-order, 10-kHz, Tschebyscheff low-pass filter with 3-dB passband ripple and a DC gain of $A_0 = 2$ has its worst case Q in the third filter section. With $Q_3 = 8.82$ and $a_3 = 0.1172$, the op amp needs to have a unity-gain bandwidth of:

$$f_T = 100 \cdot 2 \cdot \frac{10 \text{ kHz}}{0.1172} \sqrt{\frac{8.82^2 - 0.5}{8.82^2 - 0.25}} = 17 \text{ MHz}$$

In comparison, a fifth-order unity-gain, 10-kHz, Butterworth low-pass filter has a worst case Q of $Q_3 = 1.62$; $a_3 = 0.618$. Owing to the lower Q value, f_T is also lower and calculates to only:

$$f_T = 100 \cdot \frac{10 \text{ kHz}}{0.618} \sqrt{\frac{1.62^2 - 0.5}{1.62^2 - 0.25}} = 1.5 \text{ MHz}$$

Besides good DC performance, low noise, and low signal distortion, another important parameter that determines the speed of an op amp is the slew rate (SR). For adequate full-power response, the SR must be greater than:

$$SR = \pi \cdot V_{pp} \cdot f_C$$

For example, a single-supply, 100-kHz filter with 5 V_{PP} output requires an SR of at least:

$$SR = \pi \cdot 5 \text{ V} \cdot 100 \text{ kHz} = 1.57 \frac{V}{\mu s}$$

Texas Instruments offers a wide range of op amps for high-performance filters in single-supply applications. Table 16.5 provides a selection of single-supply amplifiers sorted in order of rising SR.

Table 16.5: Single-Supply Op Amp Selection Guide ($T_A = 25°C$, $V_{CC} = 5$ V)

Op Amp	Bandwidth (MHz)	Power Bandwidth (kHz)	Slew rate (V/μs)	V_{IO} (mV)	Noise (nV/Hz)
TLV2721	0.51	11	0.18	0.6	20
TLC2201A	1.8	159	2.5	0.6	8
TLV2771A	4.8	572	9	1.9	21
TLC071	10	1000	16	1.5	7
TLE2141	5.9	2800	45	0.5	10.5
THS4001	270	127 MHz (1V_{PP})	400	6	7.5

16.9 Filter Coefficient Tables

The following tables contain the coefficients for the three filter types; Bessel, Butterworth, and Tschebyscheff. The Tschebyscheff tables (Table 16.11) are split into categories for the following passband ripples: 0.5, 1, 2, and 3 dB.

The table headers consist of the following quantities:

n is the filter order,
i is the number of the partial filter,
a_i and b_i are the filter coefficients,

Table 16.6: Bessel Coefficients

n	i	a_i	b_i	$k_i = f_{Ci}/f_C$	Q_i
1	1	1.0000	0.0000	1.000	—
2	1	1.3617	0.6180	1.000	0.58
3	1	0.7560	0.0000	1.323	—
	2	0.9996	0.4772	1.414	0.69
4	1	1.3397	0.4889	0.978	0.52
	2	0.7743	0.3890	1.797	0.81
5	1	0.6656	0.0000	1.502	—
	2	1.1402	0.4128	1.184	0.56
	3	0.6216	0.3245	2.138	0.92
6	1	1.2217	0.3887	1.063	0.51
	2	0.9686	0.3505	1.431	0.61
	3	0.5131	0.2756	2.447	1.02
7	1	0.5937	0.0000	1.648	—
	2	1.0944	0.3395	1.207	0.53
	3	0.8304	0.3011	1.695	0.66
	4	0.4332	0.2381	2.731	1.13
8	1	1.1112	0.3162	1.164	0.51
	2	0.9754	0.2979	1.381	0.56
	3	0.7202	0.2621	1.963	0.71
	4	0.3728	0.2087	2.992	1.23
9	1	0.5386	0.0000	1.857	—
	2	1.0244	0.2834	1.277	0.52
	3	0.8710	0.2636	1.574	0.59
	4	0.6320	0.2311	2.226	0.76
	5	0.3257	0.1854	3.237	1.32
10	1	1.0215	0.2650	1.264	0.50
	2	0.9393	0.2549	1.412	0.54
	3	0.7815	0.2351	1.780	0.62
	4	0.5604	0.2059	2.479	0.81
	5	0.2883	0.1665	3.466	1.42

Table 16.7: Butterworth Coefficients

n	i	a_i	b_i	$k_i = f_{Ci}/f_C$	Q_i
1	1	1.0000	0.0000	1.000	—
2	1	1.4142	1.0000	1.000	0.71
3	1	1.0000	0.0000	1.000	—
	2	1.0000	1.0000	1.272	1.00
4	1	1.8478	1.0000	0.719	0.54
	2	0.7654	1.0000	1.390	1.31
5	1	1.0000	0.0000	1.000	—
	2	1.6180	1.0000	0.859	0.62
	3	0.6180	1.0000	1.448	1.62
6	1	1.9319	1.0000	0.676	0.52
	2	1.4142	1.0000	1.000	0.71
	3	0.5176	1.0000	1.479	1.93
7	1	1.0000	0.0000	1.000	—
	2	1.8019	1.0000	0.745	0.55
	3	1.2470	1.0000	1.117	0.80
	4	0.4450	1.0000	1.499	2.25
8	1	1.9616	1.0000	0.661	0.51
	2	1.6629	1.0000	0.829	0.60
	3	1.1111	1.0000	1.206	0.90
	4	0.3902	1.0000	1.512	2.56
9	1	1.0000	0.0000	1.000	—
	2	1.8794	1.0000	0.703	0.53
	3	1.5321	1.0000	0.917	0.65
	4	1.0000	1.0000	1.272	1.00
	5	0.3473	1.0000	1.521	2.88
10	1	1.9754	1.0000	0.655	0.51
	2	1.7820	1.0000	0.756	0.56
	3	1.4142	1.0000	1.000	0.71
	4	0.9080	1.0000	1.322	1.10
	5	0.3129	1.0000	1.527	3.20

Table 16.8: Tschebyscheff Coefficients for 0.5 dB

n	i	a_i	b_i	$k_i = f_{Ci}/f_C$	Q_i
1	1	1.0000	0.0000	1.000	—
2	1	1.3614	1.3827	1.000	0.86
3	1	1.8636	0.0000	0.537	—
	2	0.0640	1.1931	1.335	1.71
4	1	2.6282	3.4341	0.538	0.71
	2	0.3648	1.1509	1.419	2.94
5	1	2.9235	0.0000	0.342	—
	2	1.3025	2.3534	0.881	1.18
	3	0.2290	1.0833	1.480	4.54

Table 16.8: Tschebyscheff Coefficients for 0.5 dB—cont'd

n	i	a_i	b_i	$k_i = f_{Ci}/f_C$	Q_i
6	1	3.8645	6.9797	0.366	0.68
	2	0.7528	1.8573	1.078	1.81
	3	0.1589	1.0711	1.495	6.51
7	1	4.0211	0.0000	0.249	—
	2	1.8729	4.1795	0.645	1.09
	3	0.4861	1.5676	1.208	2.58
	4	0.1156	1.0443	1.517	8.84
8	1	5.1117	11.9607	0.276	0.68
	2	1.0639	2.9365	0.844	1.61
	3	0.3439	1.4206	1.284	3.47
	4	0.0885	1.0407	1.521	11.53
9	1	5.1318	0.0000	0.195	—
	2	2.4283	6.6307	0.506	1.06
	3	0.6839	2.2908	0.989	2.21
	4	0.2559	1.3133	1.344	4.48
	5	0.0695	1.0272	1.532	14.58
10	1	6.3648	18.3695	0.222	0.67
	2	1.3582	4.3453	0.689	1.53
	3	0.4822	1.9440	1.091	2.89
	4	0.1994	1.2520	1.381	5.61
	5	0.0563	1.0263	1.533	17.99

Table 16.9: Tschebyscheff Coefficients for 1 dB Pa

n	i	a_i	b_i	$k_i = f_{Ci}/f_C$	Q_i
1	1	1.0000	0.0000	1.000	—
2	1	1.3022	1.5515	1.000	0.96
3	1	2.2156	0.0000	0.451	—
	2	0.5442	1.2057	1.353	2.02
4	1	2.5904	4.1301	0.540	0.78
	2	0.3039	1.1697	1.417	3.56
5	1	3.5711	0.0000	0.280	—
	2	1.1280	2.4896	0.894	1.40
	3	0.1872	1.0814	1.486	5.56
6	1	3.8437	8.5529	0.366	0.76
	2	0.6292	1.9124	1.082	2.20
	3	0.1296	1.0766	1.493	8.00
7	1	4.9520	0.0000	0.202	—
	2	1.6338	4.4899	0.655	1.30
	3	0.3987	1.5834	1.213	3.16
	4	0.0937	1.0432	1.520	10.90

Table 16.9: Tschebyscheff Coefficients for 1 dB Pa—cont'd

n	i	a_i	b_i	$k_i = f_{Ci}/f_C$	Q_i
8	1	5.1019	14.7608	0.276	0.75
	2	0.8916	3.0426	0.849	1.96
	3	0.2806	1.4334	1.285	4.27
	4	0.0717	1.0432	1.520	14.24
9	1	6.3415	0.0000	0.158	—
	2	2.1252	7.1711	0.514	1.26
	3	0.5624	2.3278	0.994	2.71
	4	0.2076	1.3166	1.346	5.53
	5	0.0562	1.0258	1.533	18.03
10	1	6.3634	22.7468	0.221	0.75
	2	1.1399	4.5167	0.694	1.86
	3	0.3939	1.9665	1.093	3.56
	4	0.1616	1.2569	1.381	6.94
	5	0.0455	1.0277	1.532	22.26

Table 16.10: Tschebyscheff Coefficients for 2 dB Pa

n	i	a_i	b_i	$k_i = f_{Ci}/f_C$	Q_i
1	1	1.0000	0.0000	1.000	—
2	1	1.1813	1.7775	1.000	1.13
3	1	2.7994	0.0000	0.357	—
	2	0.4300	1.2036	1.378	2.55
4	1	2.4025	4.9862	0.550	0.93
	2	0.2374	1.1896	1.413	4.59
5	1	4.6345	0.0000	0.216	—
	2	0.9090	2.6036	0.908	1.78
	3	0.1434	1.0750	1.493	7.23
6	1	3.5880	10.4648	0.373	0.90
	2	0.4925	1.9622	1.085	2.84
	3	0.0995	1.0826	1.491	10.46
7	1	6.4760	0.0000	0.154	—
	2	1.3258	4.7649	0.665	1.65
	3	0.3067	1.5927	1.218	4.12
	4	0.0714	1.0384	1.523	14.28
8	1	4.7743	18.1510	0.282	0.89
	2	0.6991	3.1353	0.853	2.53
	3	0.2153	1.4449	1.285	5.58
	4	0.0547	1.0461	1.518	18.39

Table 16.10: Tschebyscheff Coefficients for 2 dB Pa—cont'd

n	i	a_i	b_i	$k_i = f_{Ci}/f_C$	Q_i
9	1	8.3198	0.0000	0.120	—
	2	1.7299	7.6580	0.522	1.60
	3	0.4337	2.3549	0.998	3.54
	4	0.1583	1.3174	1.349	7.25
	5	0.0427	1.0232	1.536	23.68
10	1	5.9618	28.0376	0.226	0.89
	2	0.8947	4.6644	0.697	2.41
	3	0.3023	1.9858	1.094	4.66
	4	0.1233	1.2614	1.380	9.11
	5	0.0347	1.0294	1.531	29.27

Table 16.11: Tschebyscheff Coefficients for 3 dB Pa

n	i	a_i	b_i	$k_i = f_{Ci}/f_C$	Q_i
1	1	1.0000	0.0000	1.000	—
2	1	1.0650	1.9305	1.000	1.30
3	1	3.3496	0.0000	0.299	—
	2	0.3559	1.1923	1.396	3.07
4	1	2.1853	5.5339	0.557	1.08
	2	0.1964	1.2009	1.410	5.58
5	1	5.6334	0.0000	0.178	—
	2	0.7620	2.6530	0.917	2.14
	3	0.1172	1.0686	1.500	8.82
6	1	3.2721	11.6773	0.379	1.04
	2	0.4077	1.9873	1.086	3.46
	3	0.0815	1.0861	1.489	12.78
7	1	7.9064	0.0000	0.126	—
	2	1.1159	4.8963	0.670	1.98
	3	0.2515	1.5944	1.222	5.02
	4	0.0582	1.0348	1.527	17.46
8	1	4.3583	20.2948	0.286	1.03
	2	0.5791	3.1808	0.855	3.08
	3	0.1765	1.4507	1.285	6.83
	4	0.0448	1.0478	1.517	22.87
9	1	10.1759	0.0000	0.098	—
	2	1.4585	7.8971	0.526	1.93
	3	0.3561	2.3651	1.001	4.32
	4	0.1294	1.3165	1.351	8.87
	5	0.0348	1.0210	1.537	29.00
10	1	5.4449	31.3788	0.230	1.03
	2	0.7414	4.7363	0.699	2.94
	3	0.2479	1.9952	1.094	5.70
	4	0.1008	1.2638	1.380	11.15
	5	0.0283	1.0304	1.530	35.85

Table 16.12: All-Pass Coefficients

n	i	a_i	b_i	f_i/f_C	Q_i	T_{gr0}
1	1	0.6436	0.0000	1.554	—	0.2049
2	1	1.6278	0.8832	1.064	0.58	0.5181
3	1	1.1415	0.0000	0.876	—	0.8437
	2	1.5092	1.0877	0.959	0.69	
4	1	2.3370	1.4878	0.820	0.52	1.1738
	2	1.3506	1.1837	0.919	0.81	
5	1	1.2974	0.0000	0.771	—	1.5060
	2	2.2224	1.5685	0.798	0.56	
	3	1.2116	1.2330	0.901	0.92	
6	1	2.6117	1.7763	0.750	0.51	1.8395
	2	2.0706	1.6015	0.790	0.61	
	3	1.0967	1.2596	0.891	1.02	
7	1	1.3735	0.0000	0.728	—	2.1737
	2	2.5320	1.8169	0.742	0.53	
	3	1.9211	1.6116	0.788	0.66	
	4	1.0023	1.2743	0.886	1.13	
8	1	2.7541	1.9420	0.718	0.51	2.5084
	2	2.4174	1.8300	0.739	0.56	
	3	1.7850	1.6101	0.788	0.71	
	4	0.9239	1.2822	0.883	1.23	
9	1	1.4186	0.0000	0.705	—	2.8434
	2	2.6979	1.9659	0.713	0.52	
	3	2.2940	1.8282	0.740	0.59	
	4	1.6644	1.6027	0.790	0.76	
	5	0.8579	1.2862	0.882	1.32	
10	1	2.8406	2.0490	0.699	0.50	3.1786
	2	2.6120	1.9714	0.712	0.54	
	3	2.1733	1.8184	0.742	0.62	
	4	1.5583	1.5923	0.792	0.81	
	5	0.8018	1.2877	0.881	1.42	

k_i is the ratio of the corner frequency of a partial filter, f_{Ci}, to the corner frequency of the overall filter, f_C. This ratio is used to determine the unity-gain bandwidth of the op amp, as well as to simplify the test of a filter design by measuring f_{Ci} and comparing it to f_C,

Q_i is the quality factor of the partial filter,

f_i/f_C ratio is used for test purposes of the all-pass filters, where f_i is the frequency, at which the phase is 180 degrees for a second-order filter, respectively 90 degrees for a first-order all-pass.

T_{gr0} is the normalized group delay of the overall all-pass filter.

Further Reading

[1]   D. Johnson, J. Hilburn, Rapid Practical Designs of Active Filters, John Wiley & Sons, 1975.
[2]   U. Tietze, C. Schenk, Halbleiterschaltungstechnik, Springer−Verlag, 1980.
[3]   H. Berlin, Design of Active Filters with Experiments, Howard W. Sams & Co, 1979.
[4]   M. Van Falkenburg, Analog Filter Design, Oxford University Press, 1982.
[5]   S. Franko, Design with Operational Amplifiers and Analog Integrated Circuits, McGraw−Hill, 1988.